NASA TM X-757

TECHNICAL MEMORANDUM

X-757

A METHOD FOR PREDICTING THE NORMAL-FORCE CHARACTERISTICS OF DELTA WINGS AT ANGLES OF ATTACK FROM 0° TO 90°

By David E. Fetterman

Langley Research Center
Langley Station, Hampton, Va.

[redacted]

NATIONAL AERONAUTICS AND SPACE ADMINISTRATION

WASHINGTON

March 1963

NATIONAL AERONAUTICS AND SPACE ADMINISTRATION

TECHNICAL MEMORANDUM X-757

A METHOD FOR PREDICTING THE NORMAL-FORCE CHARACTERISTICS OF DELTA WINGS AT ANGLES OF ATTACK FROM 0° TO 90°*

By David E. Fetterman

SUMMARY

A method for predicting the normal-force characteristics of delta wings of various leading-edge sweeps and radii is proposed. The method utilizes a system of three basic equations, each of which is confined to a particular angle-of-attack range definable in terms of leading-edge sweep and free-stream Mach number, and it can be applied to both flat-plate wings and those with low to moderate amounts of dihedral. Comparisons of the results with experimental data from representative configurations at supersonic and hypersonic Mach numbers indicate the method to be more generally applicable than existing theories and to have useful application at Mach numbers of greater than 3. A modification allows the prediction of the average center-line pressure coefficients for flat-plate delta wings of various sweeps with better accuracy than methods now in existence. An extension to account for the effects of arbitrary specific-heat ratio is included in the appendix.

INTRODUCTION

In order to alleviate aerodynamic heating during the reentry maneuver and to obtain a reasonably wide reentry corridor for winged vehicles, the angle-of-attack range of interest has been extended to approximately 60° to include maximum lift coefficient, and, in some proposals (ref. 1, for example), to approximately 90° to include maximum drag. As part of the overall problem of obtaining reliable predictions of the aerodynamics of vehicles over this wide angle-of-attack range, the specific problem of predicting the normal-force characteristics of wings is of fundamental concern. The basic theoretical methods, suitable for preliminary design analyses, which are available for this purpose are the linear, shock-expansion, and Newtonian theories. Of these, the linear theory, which has been extensively applied to many wing planforms, is applicable only at low supersonic speeds and from low to moderate angles of attack, since the normal-force characteristics of wings become nonlinear with angle of attack at high supersonic and hypersonic speeds. (See ref. 2.) Shock-expansion theory, which predicts this nonlinear trend with Mach number, was shown in references 3 and 4 to predict adequately the characteristics of delta wings at hypersonic speeds up to the angle

*Title, Unclassified.

of attack for leading-edge shock detachment (considered in the plane normal to the leading edge). This theory, then, is useful for two-dimensional wings or wings of relatively low leading-edge sweep. However, its range of applicability is severely limited for the highly swept delta wings of practical interest because of the low angles of attack for leading-edge shock detachment. Above angles of attack for leading-edge shock detachment, however, the semiempirical method of Post (ref. 5), and a modification of the method by Close (ref. 6), successfully predicts the force characteristics of highly swept delta wings (leading-edge sweep equals 60° or greater) at least to angles of attack of about 60°. The validity of the method when applied to wings of lower leading-edge sweep, however, has not been determined.

In lieu of more valid theories which are applicable over a 90° angle-of-attack range, the Newtonian theory is being used for hypersonic prediction purposes, and literature dealing with its application to winged configurations is being accumulated. (See ref. 7.) The Newtonian theory predicts a constant pressure coefficient over a flat surface, whereas experimental data (refs. 8 and 9) have shown that severe surface-pressure gradients, both chordwise and spanwise, exist over flat-plate delta wings at the higher angles of attack; therefore, it is reasonable to expect that this theory can give valid predictions of wing characteristics only over a restricted angle-of-attack range.

The foregoing situation is indicated by the data shown in figure 1 where experimental data, taken from unpublished data and from references 10 to 12 at a Mach number of about 6.8 for a square wing and a delta wing having a leading-edge sweep of 70°, are compared with the predictions given by the methods previously mentioned. The general disagreement between the experimental data and the predictions from all methods is evident. Although Post's method (ref. 5) and Close's modification (ref. 6) give excellent predictions of the delta-wing data throughout all but the extreme angle-of-attack range, they considerably overestimate the data for the square wing. From these comparisons, then, it is evident that no single method exists for general application over the wide angle-of-attack range currently of interest. During the analysis of the data reported in reference 12, this fact became clearly evident and led to a review of available hypersonic experimental data at a Mach number of 6.8 on delta wings of various leading-edge sweeps. The resulting analysis revealed that when properly correlated, the normal-force characteristics of delta wings in general could be expressed in a convenient mathematical form in which the predominant variables, other than angle of attack, were Mach number and leading-edge sweep. Furthermore, subsequent application of the resulting expressions to wings at both lower and higher Mach numbers verified the general applicability of the method. The purpose of this paper, then, is to present the details of this method along with determinations of its validity through comparisons with available experimental data.

SYMBOLS

A	axial force, positive rearward, -X
a_o	sonic velocity based on stagnation conditions

C	constant in linear viscosity relation, $\frac{\mu_w}{\mu} = C \frac{T_w}{T}$
C_A	axial-force coefficient, $\frac{A}{qS}$
C_N	normal-force coefficient, $\frac{N}{qS}$
C_N'	force coefficient normal to wing panel with dihedral, $\frac{N'}{qS}$
C_{N_α}	rate of change of normal-force coefficient with angle of attack at $\alpha = 0^\circ$
C_p	pressure coefficient
$C_{p,s}$	pressure coefficient corresponding to sonic velocity
$C_{p,t}$	stagnation pressure coefficient behind normal shock
c	wing root chord
M_N	normal Mach number in plane perpendicular to leading edge
M_∞	free-stream Mach number
N	normal force, positive upward, $-Z$
N'	force normal to wing panel with dihedral
p	static pressure
q	dynamic pressure
R	Reynolds number
r	leading-edge radius
S	projected planform area in X-Y plane
T	temperature
u	surface velocity
X,Y,Z	system of body coordinate axes, positive direction indicated in figure 2

x disk radial surface distance

α angle of attack, angle between flow and X axis in X-Z plane

α' true angle of attack of wing panels with dihedral, defined by equation (16)

α_i angle of attack for leading-edge shock detachment at infinite Mach number

α_{SD} angle of attack for leading-edge shock detachment at finite Mach number

$\beta = \sqrt{M_\infty^2 - 1}$

Γ dihedral angle measured in Y-Z plane (fig. 2)

γ specific-heat ratio

δ_{max} maximum flow-deflection angle at M_N

θ_{max} shock-wave angle corresponding to δ_{max} and M_N

Λ leading-edge sweep angle measured in X-Y plane (fig. 2)

μ viscosity

Subscripts:

$\mathfrak{C}_L$ center line

l lower surface

max maximum value

T tangent to oblique-shock solution

u upper surface

w wall

1 at local conditions

∞ at free-stream conditions

REVIEW OF DELTA-WING NORMAL-FORCE CHARACTERISTICS

Before giving the details of the proposed method for predicting the normal-force characteristics, it is instructive to examine first the general behavior of flat-plate delta wings in air over an angle-of-attack range from 0° to 90°, as determined by experimental investigations. Since all the theoretical methods discussed previously in the introduction overestimate the experimental data at an angle of attack of 90°, the general behavior of these delta wings at this extreme attitude is of prime importance and shall be discussed first.

Behavior at an Angle of Attack of 90°

Experimental pressure investigations on flat-plate delta wings at an angle of attack of 90°, such as those reported in references 8 and 9, have shown that pressure bleed off occurs near both the leading and trailing edges of the wings. This edge-pressure relief results in a maximum normal-force coefficient lower than the stagnation pressure coefficient behind a normal shock and accounts for the overprediction of the experimental normal-force data (fig. 1) given by modified Newtonian theory. It was shown in references 11 and 13 that the resulting maximum normal-force coefficient at hypersonic speeds is essentially constant with Mach number and, furthermore, is not affected to a great extent by planform shape. For further investigation of this result, data for flat delta wings with various leading-edge radii are shown in figure 3. (Refs. 14, 15, and 16 contain, in addition to those shown here, a wide variety of wing planforms, the maximum normal-force coefficients for which fall within the spread indicated by the respective data in fig. 3.) Allowing for data scatter among the various investigations, the data for sharp leading edges essentially confirms this conclusion. However, with blunt leading edges ($r/c \approx 0.02$), $C_{N,max}$ is significantly lowered below the sharp-edged value (compare the configurations with $\Lambda = 65^\circ$), and some effect of planform is evident (compare configurations with $\Lambda = 55^\circ$, 65°, and 75°).

The effects of edge-pressure bleed off on the maximum normal-force coefficient can be predicted by the use of experimentally determined velocity or pressure distributions over a disk, normal to the flow. This can be accomplished by the graphical disk-transformation method of Bertram and Dunavant which considers effects of planform and leading-edge radii. (See ref. 17.) For sharp leading edges, the following empirical equation derived from sharp-edged circular-disk experimental results in air was suggested by Dugan in reference 13 for wings of any planform.

$$C_{N,max} = C_{p,t}\left(0.842 + 0.158\,\frac{C_{p,s}}{C_{p,t}}\right) + \frac{1}{M_\infty{}^2} \qquad (1)$$

The term $1/M_\infty{}^2$ accounts for the average lee-surface pressure coefficient. This lee-surface pressure correction was also added to the graphical solutions and the results for $r/c = 0$ from both methods are seen to agree well with the experimental data in figure 3. The graphical method shows some effect of planform shape; however, this effect is small so that the $C_{N,max}$ for wings having any

leading-edge sweep angle and small leading-edge radii is well predicted by equation (1), which is much simpler to apply. For significantly large leading-edge radii, a simple equivalent-disk solution is not adequate, and the more laborious graphical procedure utilizing an inscribed disk with proper edge radii must be used. The reasons for this are shown by the solutions for delta wings with leading-edge radii which yield better predictions of the data for $r/c = 0.023$ than are obtained from equation (1), and which indicate that planform effects become more significant with increase in leading-edge radius. These graphical solutions were obtained from the velocity distribution curves for disks of various edge radii, normal to the flow, shown in figure 4. These curves represent experimental data collected and faired by Bertram from sources indicated in reference 18 and are essentially independent of changes in Mach number.

Disk-transformation solutions of the windward-surface maximum normal-force coefficient $\left(C_{N,l}\right)_{max}$ for delta wings with more practical leading-edge radii and sweep angles were obtained from the data of figure 4. The results are shown in figure 5, where the values of $\left(C_{N,l}\right)_{max}$ at $r/c = 0$ for all values of leading-edge sweep are assumed to be given by the solution for a disk. The effect on $\left(C_{N,l}\right)_{max}$ of planform with increasing r/c is clearly evident.

Behavior at Angles of Attack Below 90°

Over most of the angle-of-attack range, except near zero, the normal-force characteristics are determined primarily by contributions of the lower or windward surface, since the lee-side pressure coefficients at higher angle of attack are essentially constant and given to a good approximation by $-1/M_\infty^2$. (See refs. 19 and 20.) In order to examine the behavior of delta wings below an angle of attack of 90°, this lee-side normal-force contribution ($C_p = C_N$ for constant pressure) was subtracted from experimental force measurements of total C_N, obtained at a Mach number of about 6.8, for flat-plate sharp-edged delta wings having leading-edge sweep angles of 0°, 60°, and 70°. The resulting lower surface contribution $C_{N,l}$ was then normalized by $\sin^2\alpha$ and plotted against angle of attack as shown in figure 6.[1] On such a plot, the various forms of Newtonian theory would appear as constant values of $C_{N,max}$ (1.812, 2, or 2.4) over the angle-of-attack range.

From the data in figure 6, it is readily apparent that the normal-force coefficient does not vary solely as a function of $\sin^2\alpha$. Instead, a more complex variation occurs, which is further complicated by significant effects of leading-edge sweep below an angle of attack of about 70° and above the angles of attack for leading-edge shock detachment, as indicated by the intersections of Post's results with the oblique-shock solution. Below shock detachment, the data for all

[1]Unfortunately, sufficient data for flat-plate delta wings were not available to define completely the trends shown in figure 6, therefore some data for wings with dihedral are included. These data were limited to wings having maximum thickness ratios of 0.025, however, under the assumption that thickness ratios of this order would show little effects of dihedral. The overlap and continuity of the data in figure 6 support this assumption.

leading-edge sweep angles are reasonably well predicted by oblique-shock theory. Although a large amount of data scatter about the oblique-shock prediction is evident at the lower angles of attack, this scatter is to be somewhat expected because $\frac{C_{N,l}}{\sin^2\alpha}$ is very sensitive to experimental error in this angle-of-attack range. Above shock detachment, Post's method gives reasonable predictions of these data over most of the angle-of-attack range for high leading-edge sweep angles, but, as shown previously in figure 1, this method overestimates the data at low sweep angles.

An attempt was made to determine whether the data of figure 6 could be correlated in a form suitable to general mathematical definition. The form that emerged is the basis of the method of prediction which will now be discussed.

METHOD OF PREDICTION

Lower or Windward Surface

A form which conveniently correlates the data of figure 6 is shown in figure 7 as a semilog plot with $C_{N,l}/\sin^2\alpha$ as the logarithmic ordinate and $\sin\alpha$ as the abscissa. It should be noted that these parameters could also have been defined as

$$\frac{C_{N,l}}{\sin^2\alpha} = C_{D,cf}$$

and

$$\sin\alpha = \frac{M_N'}{M_\infty}$$

where $C_{D,cf}$ is the lower surface cross-flow drag coefficient at the cross-flow Mach number M_N' normal to the plane of the wing. On this type of plot, the data follow the oblique-shock theory up to the angle of attack for leading-edge shock detachment α_{SD}, above which the data correlate reasonably well with two distinct straight lines that vary according to the leading-edge sweep angle. Thus, if the equations of these separate correlating lines can be determined in general terms of Mach number and wing geometry, it is evident that the lower surface contribution to the normal-force coefficient can be calculated over the angle-of-attack range from 0° to 90° by a system of three equations, each of which applies to a particular angle-of-attack range.

The three distinct angle-of-attack ranges which are shown in figure 7 are: (1) from 0° to α_{SD}, where α_{SD} is the angle of attack for leading-edge shock

detachment at finite Mach number; (2) from α_{SD} to α_i, where α_i is the angle of attack for leading-edge shock detachment at infinite Mach number; and (3) from α_i to 90°. With leading-edge bluntness ignored, the shock-detachment angle of attack α_{SD} for flat-plate wings can be found for any Mach number from the following equations

$$\tan \alpha_{SD} = \cos \Lambda \tan \delta_{max} \tag{2}$$

$$M_\infty = \frac{M_N}{\sqrt{1 - \cos^2\alpha_{SD} \sin^2\Lambda}} \tag{3}$$

where δ_{max} is the maximum flow-deflection angle at Mach number M_N which is found from oblique-shock theory. These equations must be solved by an iterative process. By definition, $\alpha_{SD} = \alpha_i$ at $M_N = \infty$, so that equation (2) becomes

$$\tan \alpha_i = 1.012 \cos \Lambda \approx \cos \Lambda \tag{4}$$

because $\delta_{max} = 45.37^\circ$ for air.

At α_{SD} and below, the values of $C_{N,l}/\sin^2\alpha$ are obtained from oblique-shock theory or from the following approximate equation,

$$\frac{C_{N,l}}{\sin^2\alpha} = \frac{\gamma + 1}{2}\left(\frac{M_\infty}{\beta}\right)^2 + \sqrt{\left(\frac{2}{\beta \sin \alpha}\right)^2 + \left(\frac{\gamma + 1}{2}\right)^2\left(\frac{M_\infty}{\beta}\right)^4} \tag{5}$$

which was obtained from equation (4a) of reference 21 by substituting $C_N = C_p$ $\left(\text{where } C_p = \left(\frac{p_l}{p_\infty} - 1\right)\frac{2}{\gamma M_\infty^2}\right)$ and by defining K_ω in this equation by

$$K_\omega = \frac{M_\infty^2}{\beta} \sin \alpha$$

as proposed by Bertram. The variation of $C_{N,l}$ with angle of attack for various Mach numbers, as given by equation (5) with $\gamma = 1.4$, is compared in figure 8 with the predictions given by oblique-shock theory. The oblique-shock theory is seen to be well represented by equation (5) except near the maximum values of angle of attack. The results of equation (5) are also shown in figure 7, and the underprediction of oblique-shock theory is apparently a fortunate result,

because, for the case in which $\Lambda = 0^\circ$, equation (5) appears to be more representative of the experimental data than does the oblique-shock theory. This result, however, is probably due to tip effects and may be affected by wings of higher aspect ratio.

At α_i, the substitution of $M_\infty = \infty$ into equation (5) gives, for $\gamma = 1.4$,

$$\left(\frac{C_{N,l}}{\sin^2\alpha}\right)_{\alpha_i} = 2.4$$

which is the well-known "sharp leading edge" Newtonian solution.

At $\alpha = 90^\circ$, then, from the discussion in the section entitled "Behavior at Angles of Attack Below 90°," $\frac{C_{N,l}}{\sin^2\alpha}$ may be obtained for wings with relatively sharp leading edges from the following portion of equation (1)

$$\left(\frac{C_{N,l}}{\sin^2\alpha}\right)_{\alpha=90^\circ} = \left(C_{N,l}\right)_{max} = C_{p,t}\left(0.842 + 0.158\,\frac{C_{p,s}}{C_{p,t}}\right) \tag{6}$$

or, from figure 5 for a wide range of leading-edge radii. It should be noted that because of slightly different fairings of the various data for experimental sharp-edged disks, equation (6) yields a slightly higher value of $\left(C_{N,l}\right)_{max}$ than figure 5 at $r/c = 0$.

The end points of the two correlating lines having thus been determined, the equations of these lines are easily determined and the lower or windward-surface normal-force contribution can be calculated at any angle of attack above that for leading-edge shock detachment by the following equations. For $\alpha_{SD} \leqq \alpha \leqq \alpha_i$,

$$\frac{C_{N,l}}{\sin^2\alpha} = \left[\frac{\left(C_{N,l}/\sin^2\alpha_{SD}\right)^{\sin\alpha_i - \sin\alpha}}{(2.4)^{\sin\alpha_{SD} - \sin\alpha}}\right]^{\frac{1}{\sin\alpha_i - \sin\alpha_{SD}}} \tag{7}$$

where $C_{N,l}/\sin^2\alpha_{SD}$ is the value at shock detachment evaluated from equation (5). For $\alpha_i \leqq \alpha \leqq 90^\circ$,

$$\frac{C_{N,l}}{\sin^2\alpha} = \left\{\frac{(2.4)^{1 - \sin\alpha}}{\left[\left(C_{N,l}\right)_{max}\right]^{\sin\alpha_i - \sin\alpha}}\right\}^{\frac{1}{1 - \sin\alpha_i}} \tag{8}$$

Shock-Detachment Angles of Attack at or Near Zero

Although the above equations are satisfactory for most applications, equation (7) must be applied with caution in those cases when α_{SD} approaches zero. This situation will occur for very highly swept flat-plate wings and more frequently for wings with dihedral, which will be treated in a later section. (Wings with dihedral are here intended to refer to wings of the type shown in fig. 2.) For the cases in which α_{SD} is slightly greater than zero, at angles of attack above α_{SD}, equation (7) may yield unrealistic values of $C_{N,l}$ which are higher than those given by oblique-shock theory; and when $\alpha_{SD} = 0$, the solution of equation (7) is infinite. In order to obtain realistic predictions for these special cases, it is suggested that α_{SD} in equation (7) be replaced by α_T, the angle of attack at which the correlating line from α_i in figure 7 becomes tangent to the oblique-shock solution. Values of α_T may be found from

$$\sin \alpha_i = \sin \alpha_T \left[1 - \frac{\beta}{2} \frac{C_{N,l}}{\sin \alpha_T} \sqrt{1 + \left(0.6 \frac{M_\infty^2}{\beta} \sin \alpha_T \right)^2} \log_e \left(\frac{2.4}{C_{N,l} / \sin^2 \alpha_T} \right) \right] \tag{9}$$

or from figure 9, where α_T is shown as a function of α_i for various Mach numbers. For application to a specific case, this procedure should be used only when α_T is greater than α_{SD}.

Upper or Leeward Surface

The upper or leeward-surface contribution is assumed to be given by the Prandtl-Meyer expansion equations regardless of the condition of shock attachment at the leading edge. However, because of viscous effects which cause flow separation to occur from the wing leading edges on the leeward side at low angles of attack, the Prandtl-Meyer relations are invalid above the angles of attack where flow separation is first encountered. The results of references 19 and 20, as stated previously, however, indicate that the leeward pressure coefficient, after the onset of flow separation, is essentially constant over the upper surface and adequately predicted by $-1/M_\infty^2$. For the purpose here, then, it is assumed that the upper surface contribution to normal-force coefficient is given by the expansion equations up to the angle of attack at which $C_{N,u} = 1/M_\infty^2$. At all higher angles of attack, $C_{N,u}$ is constant and equal to this limiting value.

The upper surface normal-force coefficient as given by the expansion equations can be approximated by

$$\frac{C_{N,u}}{\sin^2 \alpha} = -\left[\frac{2}{\beta \sin \alpha_u} + \frac{\gamma + 1}{2} \left(\frac{M_\infty}{\beta} \right)^2 - \frac{\gamma + 1}{6} \frac{M_\infty^4}{\beta^3} \sin \alpha \right] \tag{10}$$

where α is negative for flow expansion. Equation (10) was obtained by expanding equation (25) of reference 22 in which $M\theta_e$ is replaced by $\frac{M_\infty^2}{\beta} \sin \alpha_u$. The results of equation (10) are compared with Prandtl-Meyer theory predictions in figure 10 for $\gamma = 1.4$ and 1.667. These comparisons show that within the $1/M_\infty^2$ limit the Prandtl-Meyer theory is adequately represented by equation (10).

It is believed that at the angles of attack beyond flow separation this assumption that $C_{N,u} = 1/M_\infty^2$ is valid at least up to Mach numbers of the order of 10. At higher speeds, however, the strong bow shock may increase the lee-side pressure coefficients significantly above the values given by $-1/M_\infty^2$. Unfortunately, however, insufficient data at higher Mach numbers are now available to formulate a general expression applicable to angle-of-attack, planform, and Mach number variations. Available data in air at a Mach number of 22, which will be compared later with the predictions given by the present method, indicate that these considerations of lee-side overpressure may not be important. Until further results become available, the choice of $C_{N,u} = 1/M_\infty^2$ appears to be the most realistic one available.

The total normal-force coefficient is obtained from the summation of the upper and lower surface normal-force contributions:

$$C_N = C_{N,l} + C_{N,u} \tag{11}$$

Comparison With Experimental Data at Various Mach Numbers

Comparisons of the experimental and predicted variations in the normal-force coefficient with angle of attack for wings having leading-edge sweep angles ranging from 55° to 86.5° at Mach numbers from 2.99 to 22 are shown in figure 11. (Data taken from refs. 9, 15, 16, 23, 24, and 25.) In general, these data are well predicted. However, some instances of disagreement are evident and are traceable to factors other than the failure of the method itself. In calculating the predictions, only the forces produced by the wing alone were considered, so that the overprediction of the experimental data at low angles of attack can be attributed to the neglect of the body (figs. 11(a) and (b)) or of the upper surface geometry (fig. 11(f)). The data at $M_\infty = 6.01$ (fig. 11(c)) are somewhat underpredicted. However, in comparison with the data at $M_\infty = 2.99$ and 4.00 (figs. 11(a), 11(b), and 3) for identical wings, the data at $M_\infty = 6.01$ appear to be consistently high. From the previous discussion on the behavior at high attitude, this result is contrary to what might be expected to occur; and since this result is not accounted for in reference 16, it appears that this behavior is primarily the result of data scatter among facilities. In any event, the trend of the data at $M_\infty = 6$ for various leading-edge sweep angles is well predicted.

In figure 11(g) the predictions of the variation of normal-force coefficient with angle of attack for a more practical delta-wing configuration are compared

with experimental data at Mach numbers of 8 and 22. (Data at $M = 22$ is supplied by Boeing Airplane Co.) The method gives the same prediction for both Mach numbers and is in good agreement with the experimental data. This result indicates that the lee surface has negligible effect even up to Mach numbers of 22; however, as stated previously, before this result can be considered conclusive, further experimental confirmation of this result is necessary.

Delta Wings With Dihedral

The method as previously described can be considered as a special case of a more general method applicable to wings with dihedral (fig. 2). The general method will be discussed for air in this section, and for arbitrary specific-heat ratios in the appendix.

In the angle-of-attack range from 0° to α_{SD}, the oblique-shock and expansion equations are applied in the streamwise direction so that for windward surfaces

$$\frac{(C_N)_{l,u}}{\sin^2\alpha_{l,u}} = \pm\left[\frac{\gamma+1}{2}\left(\frac{M_\infty}{\beta}\right)^2 + \sqrt{\left(\frac{2}{\beta \sin \alpha_{l,u}}\right)^2 + \left(\frac{\gamma+1}{2}\right)^2\left(\frac{M_\infty}{\beta}\right)^4}\right] \tag{12}$$

where the positive sign refers to the lower surface and the negative sign, to the upper surface, and, for example, where $(C_N)_{l,u} = C_{N,l}$ or $C_{N,u}$. The angle of attack for these surfaces in the streamwise direction is given by

$$\alpha_l = \alpha + \tan^{-1}\left(\frac{\tan\Gamma}{\tan\Lambda}\right) \tag{13}$$

and

$$\alpha_u = \tan^{-1}\left(\frac{\tan\Gamma}{\tan\Lambda}\right) - \alpha \tag{14}$$

where the sweep angle Λ and the dihedral angle Γ are defined in figure 2.

The angle of attack for leading-edge shock detachment (leading-edge bluntness ignored) at finite Mach number is obtained by iteration from equation (3), and

$$\tan\alpha_{SD} = \cos\Lambda\,\frac{\sin\Lambda\tan\delta_{max} - \tan\Gamma}{\sin\Lambda + \tan\delta_{max}\tan\Gamma} \tag{15}$$

where δ_{max} is obtained from oblique-shock theory.

At angles of attack above α_{SD} the flow must be considered in the true-angle-of-attack planes of the various wing panels. This true-angle-of-attack

plane is formed by the free-stream flow direction and the local normal to the panel surface, and thus it is similar to the angle-of-attack plane for the wing with no dihedral. The true angle of attack α', then, is the compliment of the "Newtonian" angle η, which is the angle formed by the local normal surface vector and the free-stream flow direction. From this definition, the true angle of attack is given by

$$\sin \alpha'_{l,u} = \cos \eta_{l,u} = \frac{\tan \Gamma \cos \Lambda \cos \alpha \pm \sin \Lambda \sin \alpha}{\sqrt{\tan^2 \Gamma + \sin^2 \Lambda}} \tag{16}$$

where the positive sign again applies to the lower surface and the negative sign, to the upper surface. Furthermore, since equation (16) is to be used only for windward surfaces, only zero and positive values of α'_u are to be considered.

The shock-detachment angle of attack at infinite Mach number is adequately given by

$$\tan \alpha_i = \cos \Lambda \frac{\sin \Lambda - \tan \Gamma}{\sin \Lambda + \tan \Gamma} \tag{17}$$

since $\tan \delta_{max} \approx 1$ in equation (15). Substituting α_i in equation (16) gives the true shock-detachment angle of attack α'_i.

The force coefficient normal to windward panels with dihedral C'_N is given for $\alpha_{l,SD} \leqq \alpha'_{l,u} \leqq \alpha'_i$ by

$$\frac{\left(C'_N\right)_{l,u}}{\sin^2 \alpha'_{l,u}} = \pm \left[\frac{\left(C_{N,l} / \sin^2 \alpha_{l,SD}\right)^{\sin \alpha'_i - \sin \alpha'_{l,u}}}{(2.4)^{\sin \alpha_{l,SD} - \sin \alpha'_{l,u}}} \right]^{\frac{1}{\sin \alpha'_i - \sin \alpha_{l,SD}}} \tag{18}$$

where $C_{N,l} / \sin^2 \alpha_{l,SD}$ is evaluated from equation (12) at the lower surface angle of attack for shock detachment $\alpha_{l,SD}$ which is obtained by substituting α_{SD} from equation (15) into equation (13). For the special cases where $\alpha_{l,SD}$ approaches zero, $\alpha_{l,SD}$ must be replaced in equation (18) by $\alpha_{l,T}$, which is obtained from equation (9) or figure 9 by replacing α_i by α'_i. The wing angle of attack α corresponding to $\alpha_{l,T}$ is found from equation (13).

For the true-angle-of-attack region between α'_i and 90°,

$$\frac{\left(C_N'\right)_{l,u}}{\sin^2\alpha_{l,u}'} = \pm \left\{ \frac{(2.4)^{1-\sin\alpha_{l,u}'}}{\left[\left(C_{N,l}\right)_{max}\right]^{\sin\alpha_i' - \sin\alpha_{l,u}'}} \right\}^{\frac{1}{1-\sin\alpha_i'}} \tag{19}$$

where $\left(C_{N,l}\right)_{max}$ is obtained from equation (6) for sharp leading edges or from figure 5 for blunt leading edges.

The normal-force coefficient $\left(C_N\right)_{l,u}$ for windward surfaces is then obtained from C_N' by

$$\left(C_N\right)_{l,u} = \left(C_N'\right)_{l,u} \frac{S'}{S} \cos B \tag{20}$$

where S' is the true area of the wing panel with dihedral S, the true panel area projected in the X-Y or reference-area plane, and $\cos B$, the direction cosine between the surface normal vector and the Z axis. The area ratio is

$$\frac{S'}{S} = \frac{1}{\cos\Gamma}\sqrt{1 + \tan^2\Gamma \cot^2\Lambda} \tag{21}$$

and the direction cosine is

$$\cos B = \frac{1}{\sqrt{1 + \frac{\tan^2\Gamma}{\sin^2\Lambda}}} \tag{22}$$

For wings with dihedral similar to that shown in figure 2, equation (20) reduces to

$$\left(C_N\right)_{l,u} = \left(C_N'\right)_{l,u}\sqrt{\frac{1 - \cos^2\Lambda\left(1 - \tan^2\Gamma\right)}{1 - \cos^2\Lambda\cos^2\Gamma}} \tag{23}$$

For highly swept wings, $C_N \approx C_N'$ for a large range of dihedral angles; therefore, equation (20) can usually be neglected.

For leeward surfaces, regardless of the angle-of-attack region, $C_{N,u}$ is obtained by substituting α_u from equation (14) into equation (10) and, as

previously discussed, $C_{N,u}$ is again assumed to be limited by the value $1/M_\infty^2$. The total normal-force coefficient is obtained, as before, from equation (11).[2]

Predictions obtained from the foregoing procedure of the normal-force characteristics of wings of various leading-edge sweeps and dihedrals at Mach numbers of 5, 6.8, and 8 are compared in figure 12 with experimental data taken from references 4, 24, and 26 and with unpublished data. The method is seen to give excellent predictions for all wings except for the wing with $\Gamma = 30^\circ$ (fig. 12(c)) in the medium angle-of-attack range. In spite of the failure of the method to predict this extreme case, however, it appears from these and the previous comparisons at $\Gamma = 0^\circ$ (fig. 11) that the method has useful application over wide ranges of leading-edge sweep, dihedral angle, and Mach number. For convenient reference, the pertinent equations of the method are listed in table I.

At low Reynolds numbers or high Mach numbers, or a combination of both (depending on surface temperature and the value of Lees' viscous interaction parameter $\bar{X} = \frac{M_\infty^3\sqrt{C}}{\sqrt{R}}$, ref. 21), the method should be corrected for the increase in normal-force coefficients at low angles of attack caused by boundary-layer displacement effects. Since values of $\bar{X}$ for the experimental data included herein are low for most cases,[3] these viscous effects are not significant. The effect of $\bar{X}$ on C_{N_α} for two-dimensional flat-plate wings is clearly shown in reference 27, and methods of correcting for this effect are given in references 28 and 29.

---

[2]Although not considered here, the axial-force coefficient for windward panels is given by

$$(C_A)_{l,u} = (C_N')_{l,u} \frac{S'}{S} \cos A$$

where

$$\cos A = \frac{1}{\sqrt{\sec^2\Lambda + \tan^2\Lambda \cot^2\Gamma}}$$

The total axial-force coefficient is then given by

$$C_A = C_{A,l} - C_{A,u}$$

[3]For the Boeing data at $M_\infty = 22$ (fig. 11(g)), $\bar{X}$ approached a value of 31, and significant viscous effects should have occurred at low angles of attack. However, because the contributions of the complex fuselage to normal force, which become important at these attitudes, were not considered pertinent to this report, data at these angles of attack were not included.

Average Center-Line Pressure Coefficient

The method can be modified to yield values of the average windward center-line, or asymptotic, pressure coefficients of flat-plate delta wings simply by replacing $\left(C_{N,l}\right)_{max}$ in equation (8) by $C_{p,t}$, which is approximated by the equation

$$C_{p,t} = \frac{\gamma + 3}{\gamma + 1}\left[1 - \frac{2}{(\gamma + 3)M_\infty{}^2}\right] \tag{24}$$

(See ref. 21.) The terms in equations (5) and (7), applicable below α_i, however, remained unchanged.

Predictions so obtained of the ratios of center-line pressure to free-stream pressure of wings at various Mach numbers in the low to medium angle-of-attack range are compared in figure 13 with average values obtained from reference 17. In general, the data are seen to be well predicted. Since the results of reference 8 indicate that the surface pressure gradient over a delta wing in this angle-of-attack range is essentially zero, except in regions near blunt leading edges, the method can also be confidently applied to regions other than the center line. At angles of attack above the onset of subsonic flow (about 55°), however, references 8 and 9 also indicate that the flow over the windward surface of flat-plate delta wings becomes three dimensional and that severe surface gradients, both chordwise and spanwise, exist. Prediction methods, such as the present one, which neglect this three-dimensional nature of the flow are, therefore, inadequate for overall application in this high angle-of-attack region. Depending on the degree of surface pressure gradients for a particular case, however, such methods may be useful over a reasonably large but limited region of the wing.

In order to test the present method in the high angle-of-attack region, the predictions of the center-line pressure coefficient are compared in figure 14 with experimental values at various chordwise stations on delta wings of various sweep angles. Also shown in this figure are similar predictions given by the modified Newtonian theory and the 5-term approximation developed by Love in the appendix of reference 20. It is seen that for all values of leading-edge sweep the present method gives reasonably good predictions of the center-line pressure coefficients except those near the wing apex. These coefficients, however, should not be considered asymptotic inasmuch as they are affected to an important extent by leading-edge bluntness at medium angles of attack and by edge-pressure bleed off at extreme angles of attack. At the lower values of leading-edge sweep ($\Lambda = 50°$), Love's 5-term approximation gives better predictions of the data near the wing apex; however, the method tends to overpredict significantly these and the more rearward data throughout most of the angle-of-attack range as leading-edge sweep is increased. Modified Newtonian theory, in general, appears to be inadequate except, of course, for extreme sweep angles. As shown in reference 30, this theory becomes essentially exact for the special case of $\Lambda = 90°$ (cylinder).

CONCLUDING REMARKS

A method has been proposed for predicting the normal-force characteristics of delta wings by a system of equations, each of which is applicable over a particular angle-of-attack range definable in terms of leading-edge sweeps and radii and free-stream Mach number. Comparisons of the predictions, so obtained, with experimental results from various sources indicate the method to be more generally applicable than existing methods and to have useful application above Mach numbers of at least 3 for a wide range of leading-edge sweep and dihedral angles. An extension of this method allows the average center-line, or asymptotic, pressure coefficient of flat-plate delta wings or of those with small dihedral and various leading-edge sweep angles to be predicted with better accuracy than methods previously available.

Langley Research Center,
National Aeronautics and Space Administration,
Langley Station, Hampton, Va., November 9, 1962.

APPENDIX

EXTENSION OF THE METHOD TO INCLUDE OTHER VALUES OF SPECIFIC-HEAT RATIO

In the angle-of-attack region between 0° and α_{SD}, the pertinent equations (12) to (14) for windward surfaces contain variable γ terms and need no further discussion.

The angle of attack for leading-edge shock detachment at finite Mach number α_{SD} can be found from equation (15) where, from oblique-shock theory,

$$\frac{1}{\tan \delta_{max}} = \tan \theta_{max}\left[\frac{(\gamma + 1)M_\infty{}^2}{2\left(M_\infty{}^2 \sin \theta_{max} - 1\right)} - 1\right] \tag{A1}$$

where

$$\sin^2\theta_{max} = \frac{1}{\gamma M_\infty{}^2}\left[M_\infty{}^2 \frac{\gamma + 1}{4} - 1 + \sqrt{(\gamma + 1)\left(1 + \frac{\gamma - 1}{2} M_\infty{}^2 + \frac{\gamma + 1}{6} M_\infty{}^4\right)}\right] \tag{A2}$$

When $M_\infty = \infty$,

$$\tan \delta_{max} = \frac{1}{\sqrt{(\gamma - 1)(\gamma + 1)}}$$

α_i is given by

$$\tan \alpha_i = \cos \Lambda \frac{\sin \Lambda - \sqrt{(\gamma - 1)(\gamma + 1)} \tan \Gamma}{\sqrt{(\gamma - 1)(\gamma + 1)} \sin \Lambda + \tan \Gamma} \tag{A3}$$

and α_i' is obtained by substituting values of α_i into equation (16).

In the true-angle-of-attack region between $\alpha_{l,SD}$ and α_i', the force coefficient normal to windward surface is given by

$$\frac{\left(C_N'\right)_{l,u}}{\sin^2\alpha_{l,u}'} = \pm \left[\frac{\left(C_{N,l}/\sin^2\alpha_{l,SD}\right)^{\sin\alpha_i' - \sin\alpha_{l,u}'}}{(\gamma+1)^{\sin\alpha_{l,SD} - \sin\alpha_{l,u}'}} \right]^{\frac{1}{\sin\alpha_i' - \sin\alpha_{l,SD}}} \tag{A4}$$

where, for the special cases when $\alpha_{l,SD} \to 0$, $\alpha_{l,T}$ is substituted for $\alpha_{l,SD}$ and is obtained from

$$\sin\alpha_i' = \sin\alpha_{l,T}\left[1 - \frac{\beta}{2}\frac{C_{N,l}}{\sin\alpha_{l,T}}\sqrt{1 + \left(\frac{\gamma+1}{4}\frac{M_\infty^2}{\beta}\sin\alpha_{l,T}\right)^2}\,\log_e\left(\frac{\gamma+1}{C_{N,l}/\sin^2\alpha_{l,T}}\right)\right] \tag{A5}$$

At Mach numbers in excess of 10, this expression can be adequately approximated by

$$\sin\alpha_{l,T} \approx \frac{2}{3}\alpha_i'$$

Again for windward surfaces, in the true-angle-of-attack range between α_i' and 90°,

$$\frac{\left(C_N'\right)_{l,u}}{\sin^2\alpha_{l,u}'} = \pm \left\{ \frac{(\gamma+1)^{1-\sin\alpha_{l,u}'}}{\left[\left(C_{N,l}\right)_{max}\right]^{\sin\alpha_i' - \sin\alpha_{l,u}'}} \right\}^{\frac{1}{1-\sin\alpha_i'}} \tag{A6}$$

For wings with relatively sharp leading edges,

$$\left(C_{N,l}\right)_{max} = \frac{(\gamma+3)M_\infty^2 - 2}{(\gamma+1)M_\infty^2}\left\{0.842 - 0.158\left(\frac{2}{\gamma+1}\right)^{\frac{\gamma}{\gamma-1}}\left[\frac{\gamma M_\infty^2(\gamma+3) - (3\gamma-1)}{\gamma M_\infty^2(\gamma+3) - 2\gamma}\right]\right\} \tag{A7}$$

which for high Mach numbers reduces to

$$\left(C_{N,l}\right)_{max} = \frac{\gamma + 3}{\gamma + 1}\left[0.842 - 0.158\left(\frac{2}{\gamma + 1}\right)^{\frac{\gamma}{\gamma-1}}\right] \tag{A8}$$

The normal-force coefficient $\left(C_N\right)_{l,u}$ for windward surfaces at angles of attack above α_{SD} is then found by substituting values of $\left(C'_N\right)_{l,u}$, obtained from equations (A4) and (A6), into equations (20) to (23) and (11).

For the leeward surfaces, $C_{N,u}$, again assumed to be limited by $1/M_\infty{}^2$, is given by equation (10) with appropriate corrections made to the α terms for wings with dihedral by use of equation (14).

The center-line pressure coefficient is obtained by substituting $C_{p,t}$ (obtained from eq. (24)) for $\left(C_{N,l}\right)_{max}$ in equation (A6).

It should be noted that equation (A7) was obtained simply by expressing equation (6) in terms of γ. This generalization is valid only if the experimental pressure distribution over a disk, normal to the flow, in a general flow medium varies similarly to that which occurs in air. At a Mach number of 22 in helium ($\gamma = 1.667$), equation (A7) yields a value of $\left(C_{N,l}\right)_{max} = 1.608$. This value can be compared with experimental force results from reference 31 and from unpublished tests in the Langley helium tunnels. These results indicate that values of the axial-force coefficient C_A for flat-faced cylinders (flat face normal to the flow) of various fineness ratios f_n range from $C_A = 1.51$ for $f_n = 0.5$ to $C_A = 1.68$ for $f_n = 4$. The measurements on the larger fineness-ratio body include cylinder-skin friction drag and low induced pressures over the base, whereas, the low fineness-ratio measurements include high induced pressures over the base and small skin friction drag; thus, the intermediate calculated value of 1.608 from equation (A7), for the windward surface alone, appears to be a reasonable estimate and infers this similarity in disk pressure distributions.

Unfortunately, no experimental data for specific-heat ratios other than 1.4 exist on delta wings at sufficiently high angles of attack for the evaluation of this extension of the method to include variable γ. Some experimental data on delta wings have been obtained in helium; however, the angles of attack are limited to 20° or less so that only the shock-expansion portion of the method can be evaluated. Since the validity of this theory has already been adequately proven (see ref. 28), additional confirmation of this portion of the method is not necessary here. It is interesting to note, however, that with the substitution of $\gamma = 1$ and $M_\infty = \infty$ into equations (A5) and (A6), the method collapses into the single equation

$$\frac{C_N}{\sin^2\alpha} = 2$$

which agrees with exact Newtonian theory.

REFERENCES

1. Staff of Langley Flight Research Division (Compiled by Donald C. Cheatham): A Concept of a Manned Satellite Reentry Which Is Completed With a Glide Landing. NASA TM X-226, 1959.

2. Fetterman, David E., and Ridyard, Herbert W.: The Effect of a Change in Airfoil Section on the Hinge-Moment Characteristics of a Half-Delta Tip Control With a 60° Sweep Angle at a Mach Number of 6.9. NACA RM L54H16a, 1954.

3. Bertram, Mitchel H., and McCauley, William D.: Investigation of the Aerodynamic Characteristics at High Supersonic Mach Numbers of a Family of Delta Wings Having Double-Wedge Sections With the Maximum Thickness at 0.18 Chord. NACA RM L54G28, 1954.

4. Bertram, Mitchel H., and McCauley, William D.: An Investigation of the Aerodynamic Characteristics of Thin Delta Wings With a Symmetrical Double-Wedge Section at a Mach Number of 6.9. NACA RM L55B14, 1955.

5. Post, J.: Lift and Drag-Due-to-Lift of Thin Delta Wings at Hypersonic Speeds and High Angles of Attack. SR-126-TM-A-6, CONVAIR.

6. Close, William H.: Hypersonic Longitudinal Trim, Stability, and Control Characteristics of a Delta-Wing Configuration at High Angles of Attack. NASA TM X-240, 1960.

7. Olstad, Walter B.: Theoretical Evaluation of Hypersonic Forces, Moments, and Stability Derivatives for Combinations of Flat Plates, Including Effects of Blunt Leading Edges, by Newtonian Impact Theory. NASA TN D-1015, 1962.

8. Dunavant, James C.: Investigation of Heat Transfer and Pressures on Highly Swept Flat and Dihedraled Delta Wings at Mach Numbers of 6.8 and 9.6 and Angles of Attack to 90°. NASA TM X-688, 1962.

9. Clark, E. L., and Spurlin, C. J.: The Aerodynamic Characteristics of a 75-Deg Swept Delta Wing at High Angles of Attack and Mach Numbers of 2 to 8. AEDC-TDR-62-99 (Contract No. AF 40(600)-800 S/A 24(61-73)), Arnold Eng. Dev. Center, May 1962.

10. McLellan, Charles H., Bertram, Mitchel H., and Moore, John A.: An Investigation of Four Wings of Square Plan Form at a Mach Number of 6.9 in the Langley 11-Inch Hypersonic Tunnel. NACA Rep. 1310, 1957. (Supersedes NACA RM L51D17.)

11. Penland, Jim A., and Armstrong, William O.: Static Longitudinal Aerodynamic Characteristics of Several Wing and Blunt-Body Shapes Applicable for Use as Reentry Configurations at a Mach Number of 6.8 and Angles of Attack up to 90°. NASA TM X-65, 1959.

12. Fetterman, David E., and Neal, Luther, Jr.: An Analysis of the Delta-Wing Hypersonic Stability and Control Behavior at Angles of Attack Between 30° and 90°. NASA TN D-1602, 1963.

13. Dugan, Duane W.: Estimation of Static Longitudinal Stability of Aircraft Configurations at High Mach Numbers and at Angles of Attack Between 0° and ±180°. NASA MEMO 1-17-59A, 1959.

14. Foster, Gerald V.: Longitudinal Aerodynamic Characteristics at a Mach Number of 1.97 of a Series of Related Winged Reentry Configurations for Angles of Attack From 0° to 90°. NASA TM X-461, 1961.

15. Smith, Fred M., and Nichols, Frank H., Jr.: A Wind-Tunnel Investigation of the Aerodynamic Characteristics of a Generalized Series of Winged Reentry Configurations at Angles of Attack to 180° at Mach Numbers of 2.38, 2.99, and 4.00. NASA TM X-512, 1961.

16. Hondros, James G., and Goldberg, Theodore J.: Aerodynamic Characteristics of a Group of Winged Reentry Vehicles at Mach Number 6.01 at Angles of Attack From 60° to 120° and -10° to 30° Roll at 90° Angle of Attack. NASA TM X-511, 1961.

17. Bertram, Mitchel H., and Henderson, Arthur, Jr.: Recent Hypersonic Studies of Wings and Bodies. ARS Jour., vol. 31, no. 8, Aug. 1961, pp. 1129-1139.

18. Bertram, M. H., and Everhart, P. E.: An Experimental Study of the Pressure and Heat-Transfer Distribution on a 70° Sweep Slab Delta Wing in Hypersonic Flow. NASA TR R-153, 1963.

19. Mayer, John P.: A Limit Pressure Coefficient and an Estimation of Limit Forces on Airfoils at Supersonic Speeds. NACA RM L8F23, 1948.

20. Mueller, James N. (With appendix by Eugene S. Love): Pressure Distributions on Blunt Delta Wings at a Mach Number of 2.91 and Angles of Attack up to 90°. NASA TM X-623, 1962.

21. Lees, Lester: Hypersonic Flow. Fifth International Aeronautical Conference (Los Angeles, Calif., June 20-23, 1955), Inst. Aero. Sci., Inc., 1955, pp. 241-276.

22. Linnell, Richard D.: Two-Dimensional Airfoils in Hypersonic Flows. Jour. Aero. Sci., vol. 16, no. 1, Jan. 1949, pp. 22-30.

23. Putnam, Lawrence E., and Brooks, Cuyler W., Jr.: Static Longitudinal Aerodynamic Characteristics at a Mach Number of 10.03 of Low-Aspect-Ratio Wing-Body Configurations Suitable for Reentry. NASA TM X-733, 1962.

24. Onspaugh, Carl M., and Sullivan, Phillip J.: Study To Determine Aerodynamic Characteristics on Hypersonic Re-Entry Configurations. Pt. I - Experimental Phase. Vol. 3 - Experimental Report - Mach Number 8. WADD Tech. Rep. 61-56, Pt. I, Vol. 3, U.S. Air Force, Mar. 1961.

25. Clark, E. L., and Spurlin, C. J.: Force Tests of the AD-599I-1 Dyna-Soar Model at Mach Number 8. AEDC-TN-61-145 (Contract No. AF 40(600)-800 S/A 24(61-73)), Arnold Eng. Dev. Center, Nov. 1961.

26. Rockhold, Vernon G., Onspaugh, Carl M., and Marcy, William L.: Study to Determine Aerodynamic Characteristics on Hypersonic Re-Entry Configurations. Pt. I - Experimental Phase. Vol. 2 - Experimental Report - Mach Number 5. WADD Tech. Rep. 61-56, Pt. I, Vol. 2, U.S. Air Force, Mar. 1961.

27. Bertram, Mitchel H., and Henderson, Arthur, Jr.: Effects of Boundary-Layer Displacement and Leading-Edge Bluntness on Pressure Distribution, Skin Friction, and Heat Transfer of Bodies at Hypersonic Speeds. NACA TN 4301, 1958.

28. White, Frank M., Jr.: Hypersonic Laminar Viscous Interactions on Inclined Flat Plates. ARS Jour. (Tech. Notes), vol. 32, no. 5, May 1962, pp. 780-781.

29. Francis, W. Leon, Malvestuto, Frank S., Jr., Stuart, Jay W., Jr.: Study To Determine Skin-Friction Drag in Hypersonic Low-Density Flow - vol. I: Summary Analysis. Tech. Rep. No. ASD-TR-61-433, vol. I, Apr. 1962.

30. Penland, Jim A.: Aerodynamic Characteristics of a Circular Cylinder at Mach Number 6.86 and Angles of Attack up to 90°. NACA TN 3861, 1957. (Supersedes NACA RM L54A14.)

31. Henderson, Arthur, Jr.: Recent Investigations of the Aerodynamic Characteristics of General and Specific Lifting and Nonlifting Configurations at Mach 24 in Helium, Including Air-Helium Simulation Studies. Presented at the Specialists' Meeting on the High Temperature Aspects of Hypersonic Flow (Rhode-Saint-Genese, Belgium), AGARD, Apr. 1962.

TABLE I.- SUMMARY OF EQUATIONS

$[\gamma = 1.4]$

<table>
<tr><td colspan="3">Windward surfaces</td></tr>
<tr><td colspan="3">Angle-of-attack range</td></tr>
<tr><td>$0 \leqq \alpha_{l,u} \leqq \alpha_{l,SD}$</td><td>$\alpha_{l,SD} \leqq \alpha'_{l,u} \leqq \alpha'_i$</td><td>$\alpha'_i \leqq \alpha'_{l,u} \leqq 90^\circ$</td></tr>
<tr><td>$\dfrac{(C_N)_{l,u}}{\sin^2\alpha_{l,u}} = \pm\left[1.2\left(\dfrac{M_\infty}{\beta}\right)^2 + \sqrt{\left(\dfrac{2}{\beta \sin \alpha_{l,u}}\right)^2 + 1.44\left(\dfrac{M_\infty}{\beta}\right)^4}\right]$
where α_l is obtained from equation (13),
α_u, from equation (14),
and α_{SD}, from equations (3) and (15).</td><td>$\dfrac{(C'_N)_{l,u}}{\sin^2\alpha'_{l,u}} = \pm\left[\dfrac{\left(C_{N,l}/\sin^2\alpha_{l,SD}\right)^{\sin\alpha'_i - \sin\alpha'_{l,u}}}{(2.4)^{\sin\alpha_{l,SD} - \sin\alpha'_{l,u}}}\right]^{\frac{1}{\sin\alpha'_i - \sin\alpha_{l,SD}}}$
where $\alpha'_{l,u}$ is obtained from equation (16),
and α'_i from equations (16) and (17).
For $\alpha_{l,SD} \to 0$, where $\alpha_{l,SD}$ is replaced by $\alpha_{l,T}$,
$\alpha_{l,T}$ is obtained from figure 9,
α for $\alpha_{l,T}$, from equation (13),
and $(C_N)_{l,u}$, from equation (20).</td><td>$\dfrac{(C'_N)_{l,u}}{\sin^2\alpha'_{l,u}} = \pm\left\{\dfrac{(2.4)^{1-\sin\alpha'_{l,u}}}{\left[(C_{N,l})_{max}\right]^{\sin\alpha'_i - \sin\alpha'_{l,u}}}\right\}^{\frac{1}{1-\sin\alpha'_i}}$
where $(C_{N,l})_{max}$ is obtained from equation (6) or figure 5,
and $(C_N)_{l,u}$ from equation (20).</td></tr>
<tr><td colspan="3">Leeward surfaces</td></tr>
<tr><td colspan="3">$C_{N,u} = -\left[\dfrac{2}{\beta \sin \alpha_u} + 1.2\left(\dfrac{M_\infty}{\beta}\right)^2 - 0.4\,\dfrac{M_\infty^4}{\beta^3}\sin\alpha_u\right]$
where $C_{N,u} \leqq \dfrac{1}{M_\infty^2}$
and α_u is obtained from equation (14).
When α is greater than that for $C_{N,u} = \dfrac{1}{M_\infty^2}$, then $C_{N,u}$ is taken as constant at the value $\dfrac{1}{M_\infty^2}$.</td></tr>
<tr><td colspan="3">Total wing</td></tr>
<tr><td colspan="3">$C_N = C_{N,l} + C_{N,u}$</td></tr>
</table>

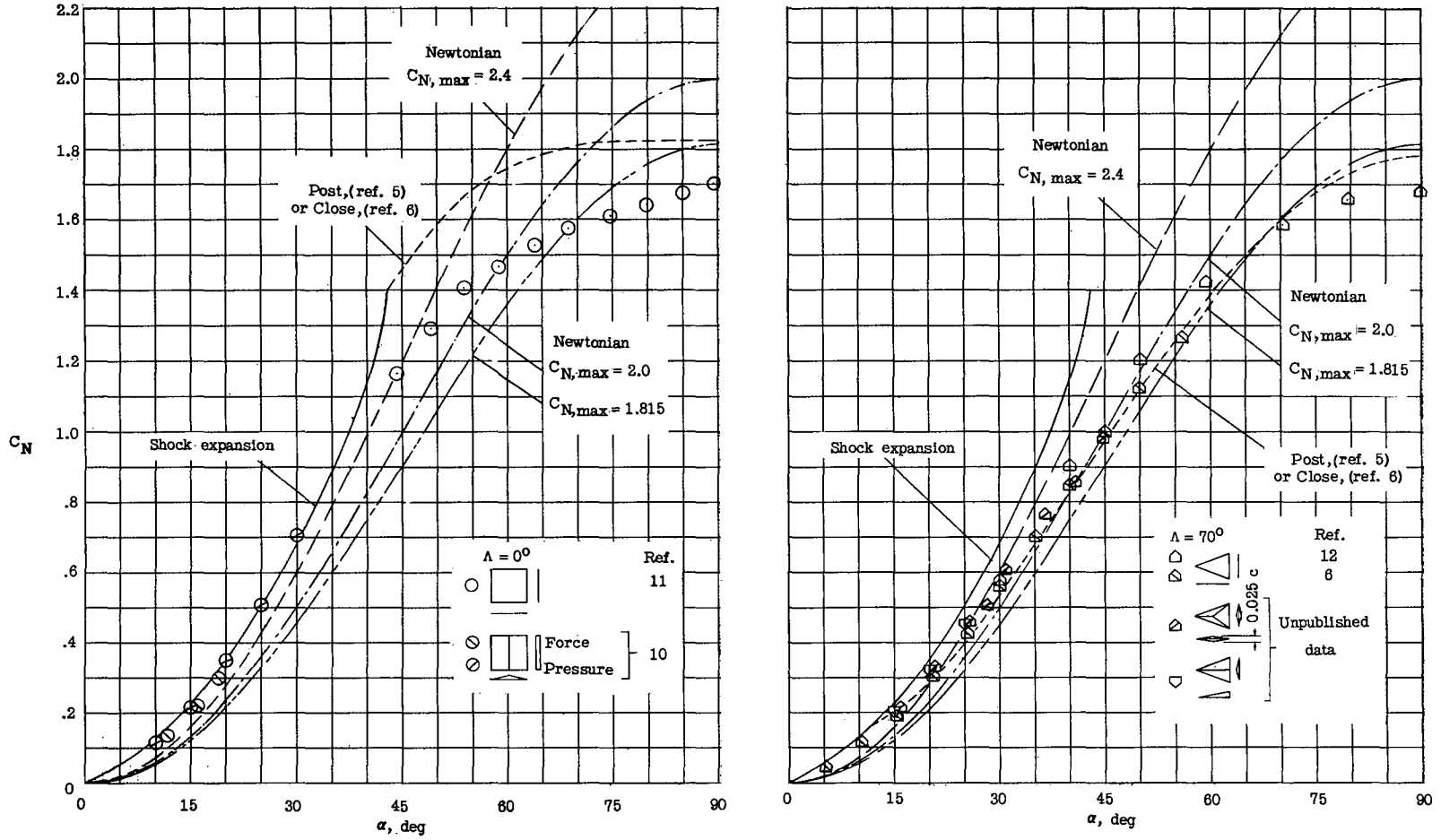

Figure 1.- Comparison of experimental and predicted variation of normal-force coefficient with angle of attack at $M_\infty = 6.8$.

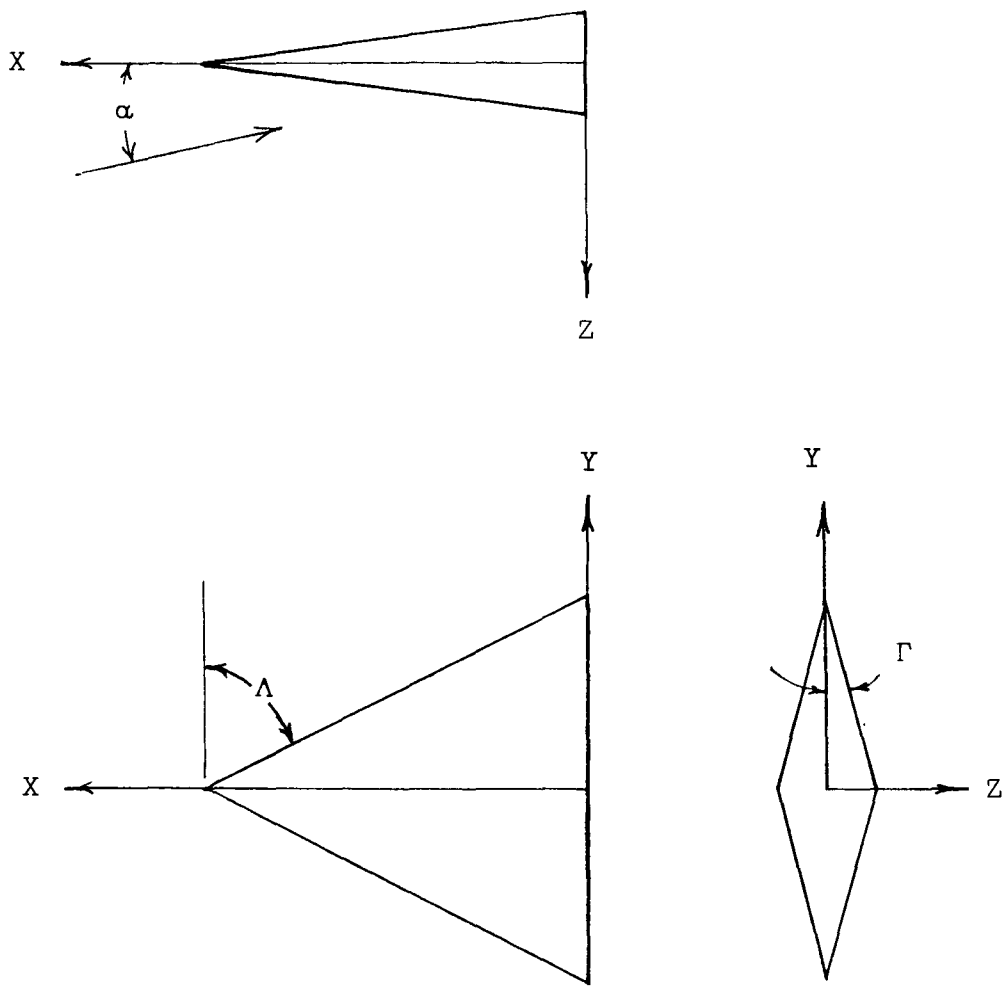

Figure 2.- Angle definitions for wings with dihedral.

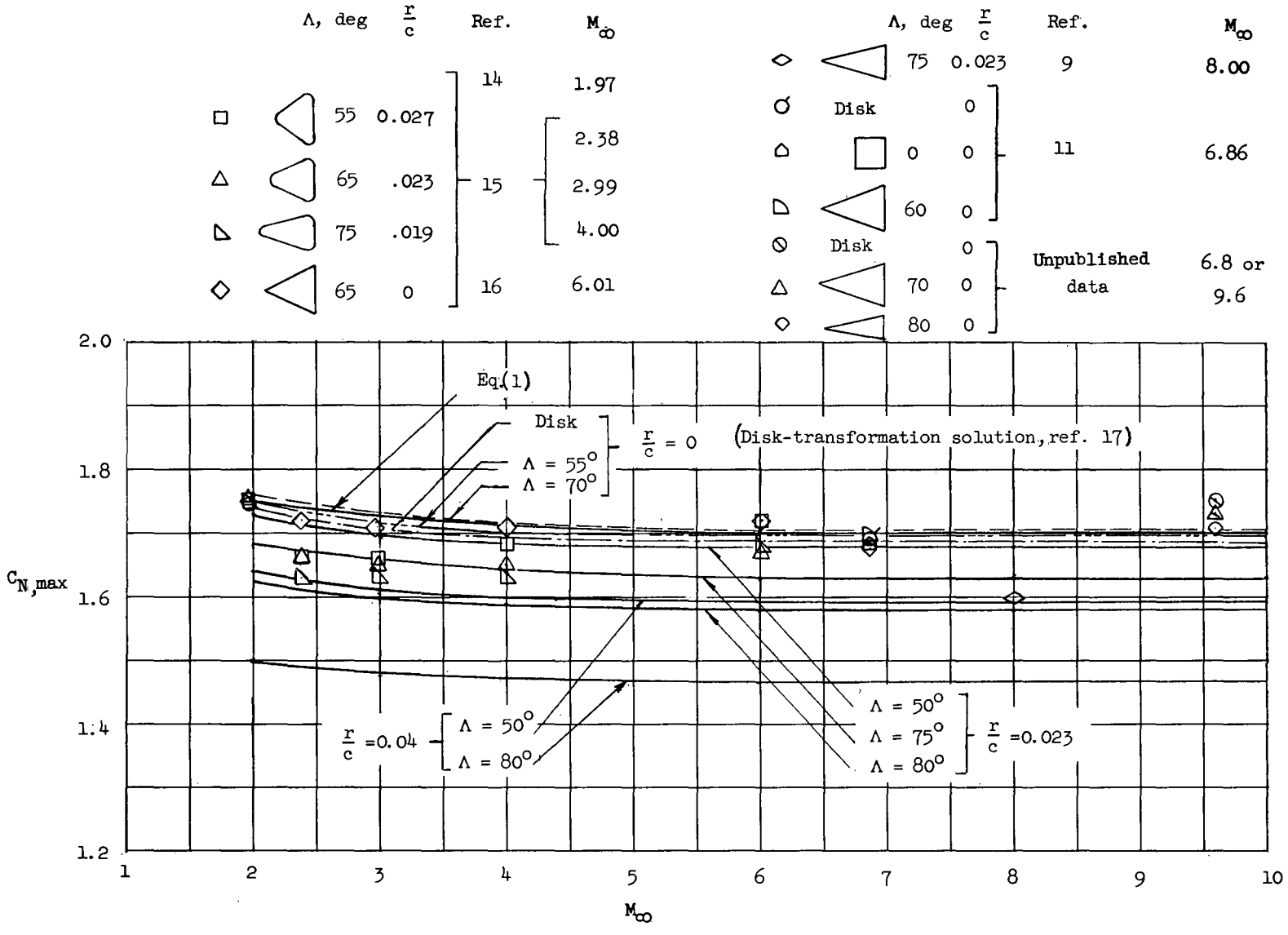

Figure 3.- Effect of wing planform and Mach number on normal-force coefficient at $\alpha = 90^{\circ}$.

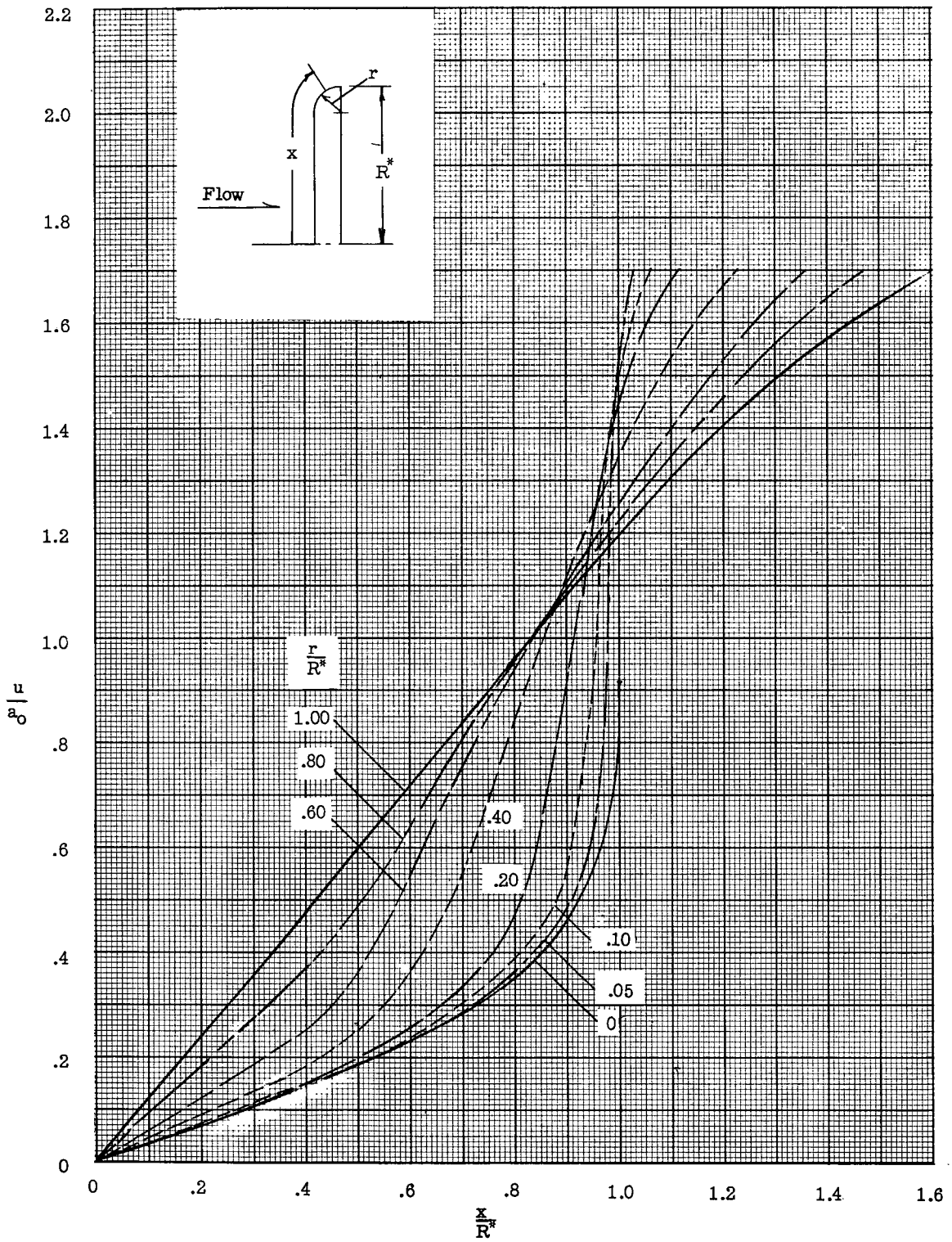

Figure 4.- Velocity distribution over a disk, normal to flow, with various edge radii.

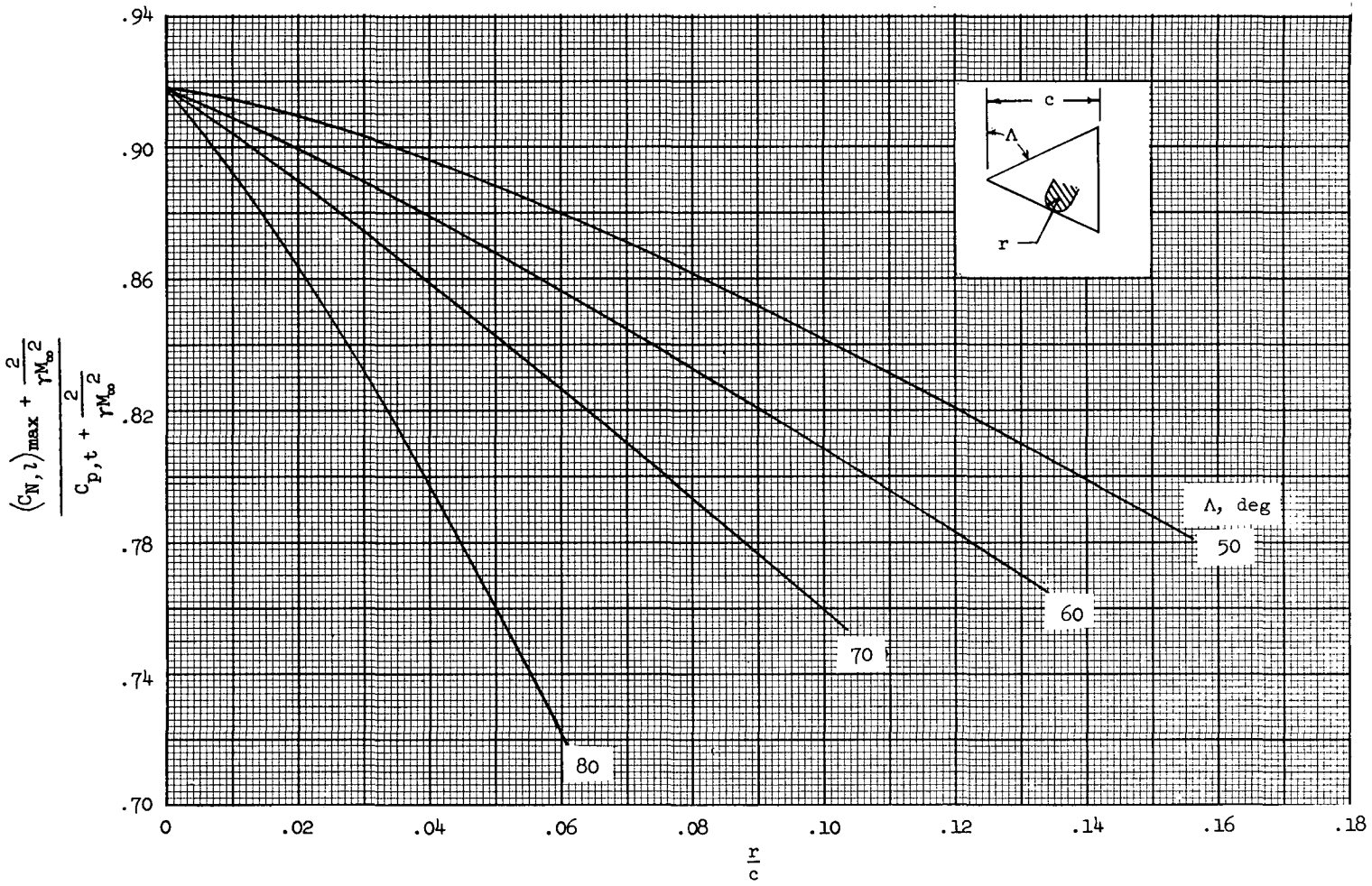

Figure 5.- Windward-surface maximum normal-force coefficients for flat-plate delta wings of various leading-edge radii and sweep angles obtained from the disk-transformation method of reference 17.

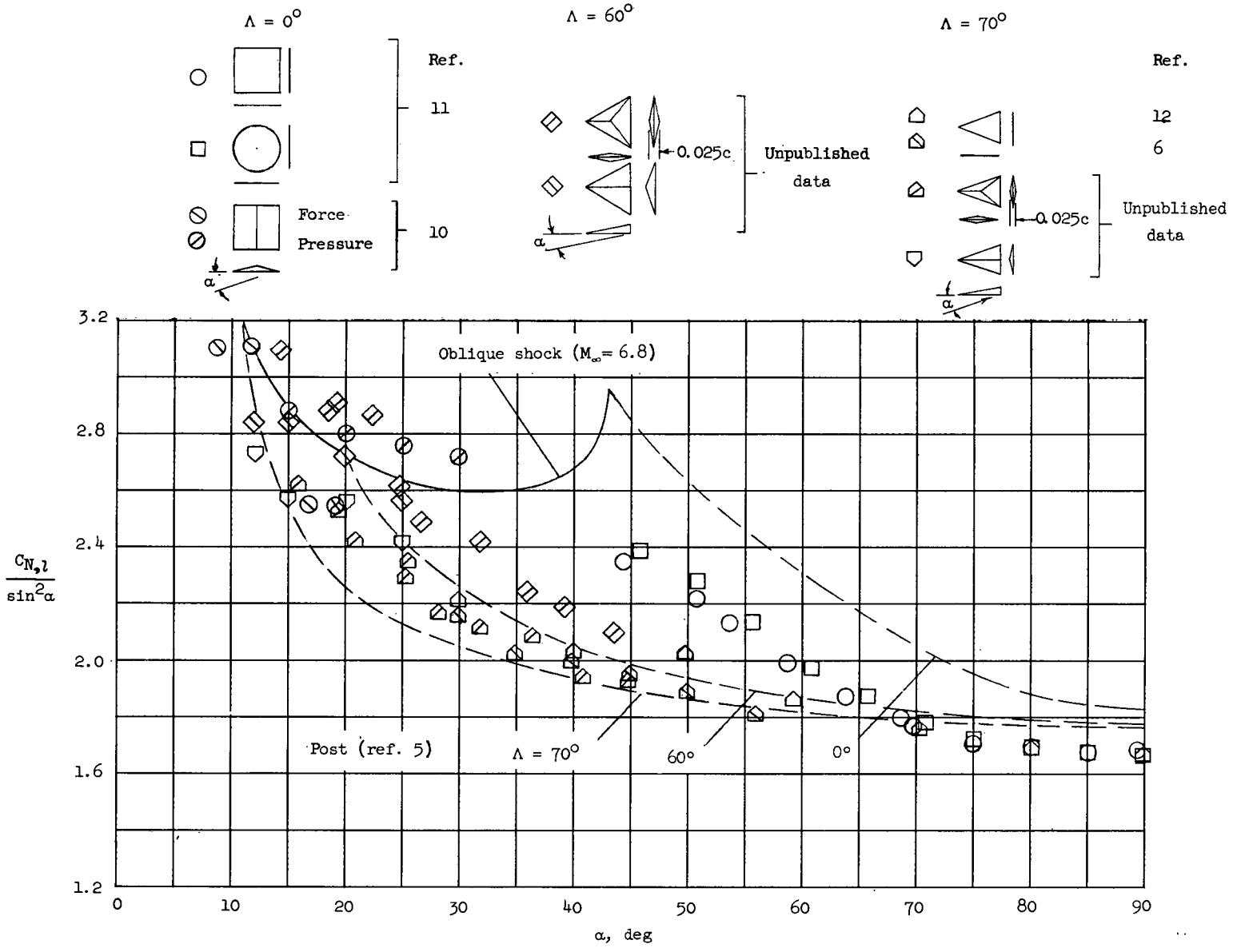

Figure 6.- Variation of lower surface normal-force coefficient, normalized by $\sin^2\alpha$, with angle of attack for delta wings of various leading-edge sweep. $M_\infty = 6.86$.

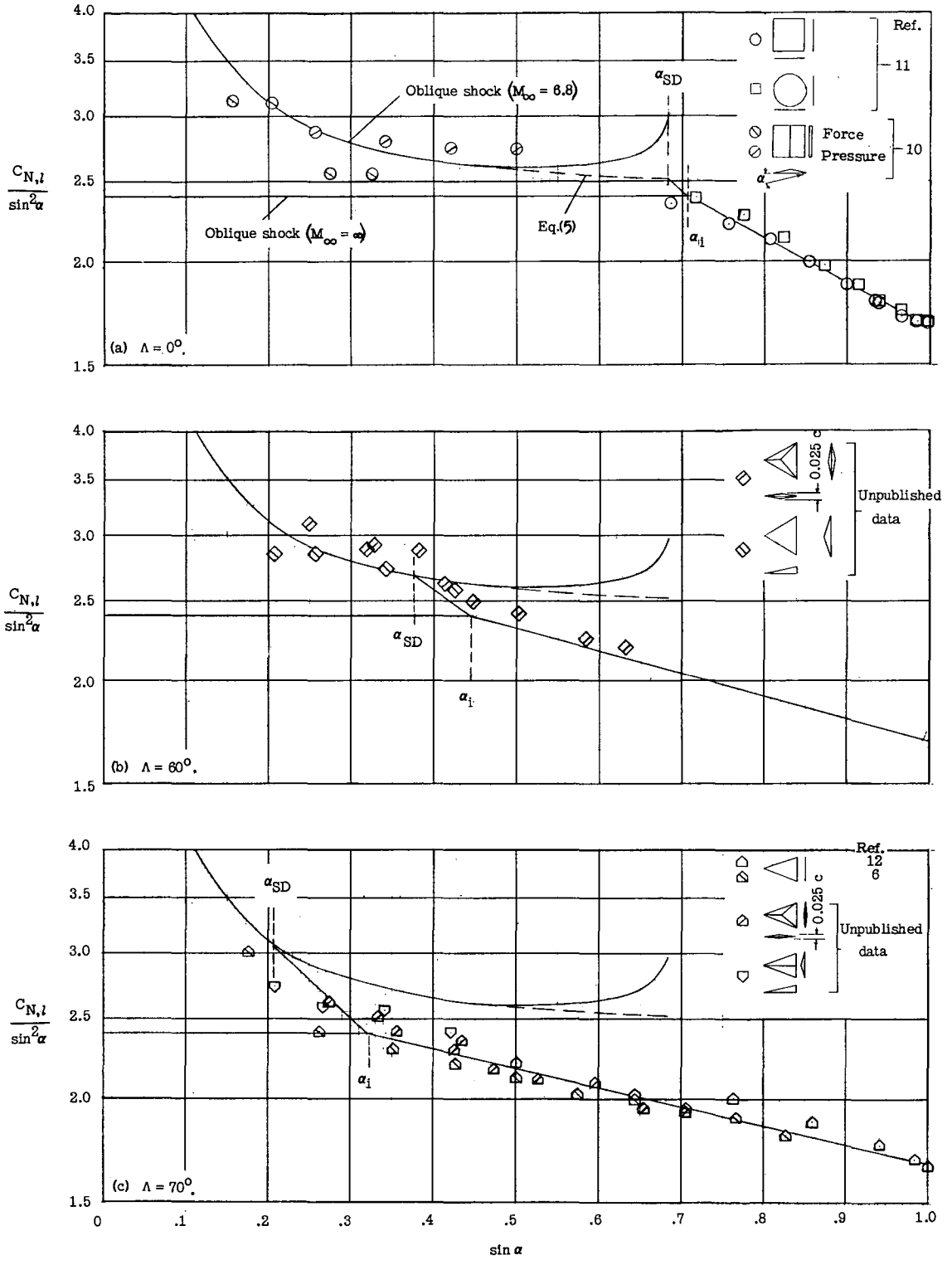

Figure 7.- Correlation curves for $C_{N,l}/\sin^2\alpha$ for wings of various leading-edge sweeps. $M_\infty = 6.86$.

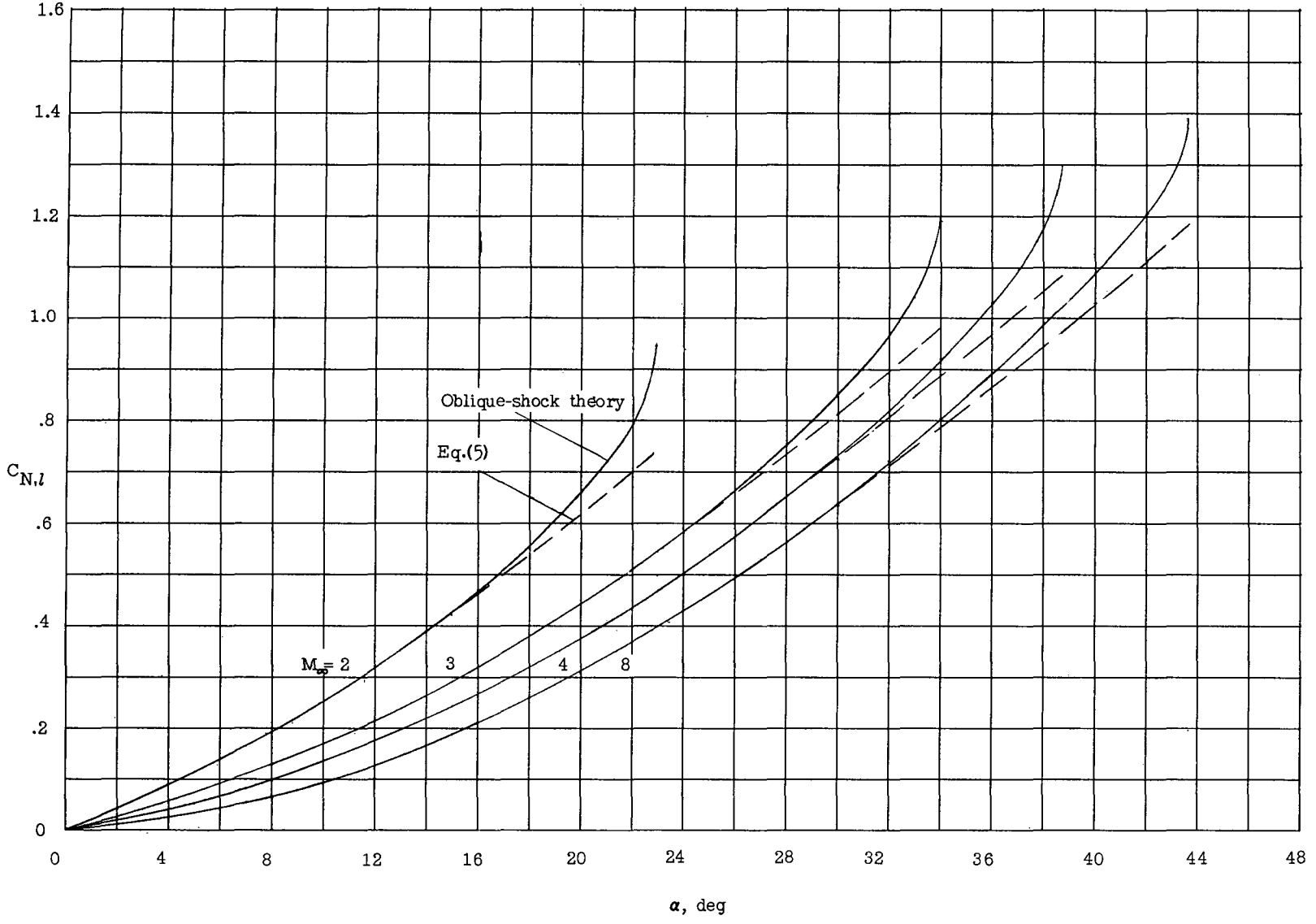

Figure 8.- Comparison of exact and approximate predictions of variation of two-dimensional flat-plate lower surface normal-force coefficient with angle of attack. $\gamma = 1.4$.

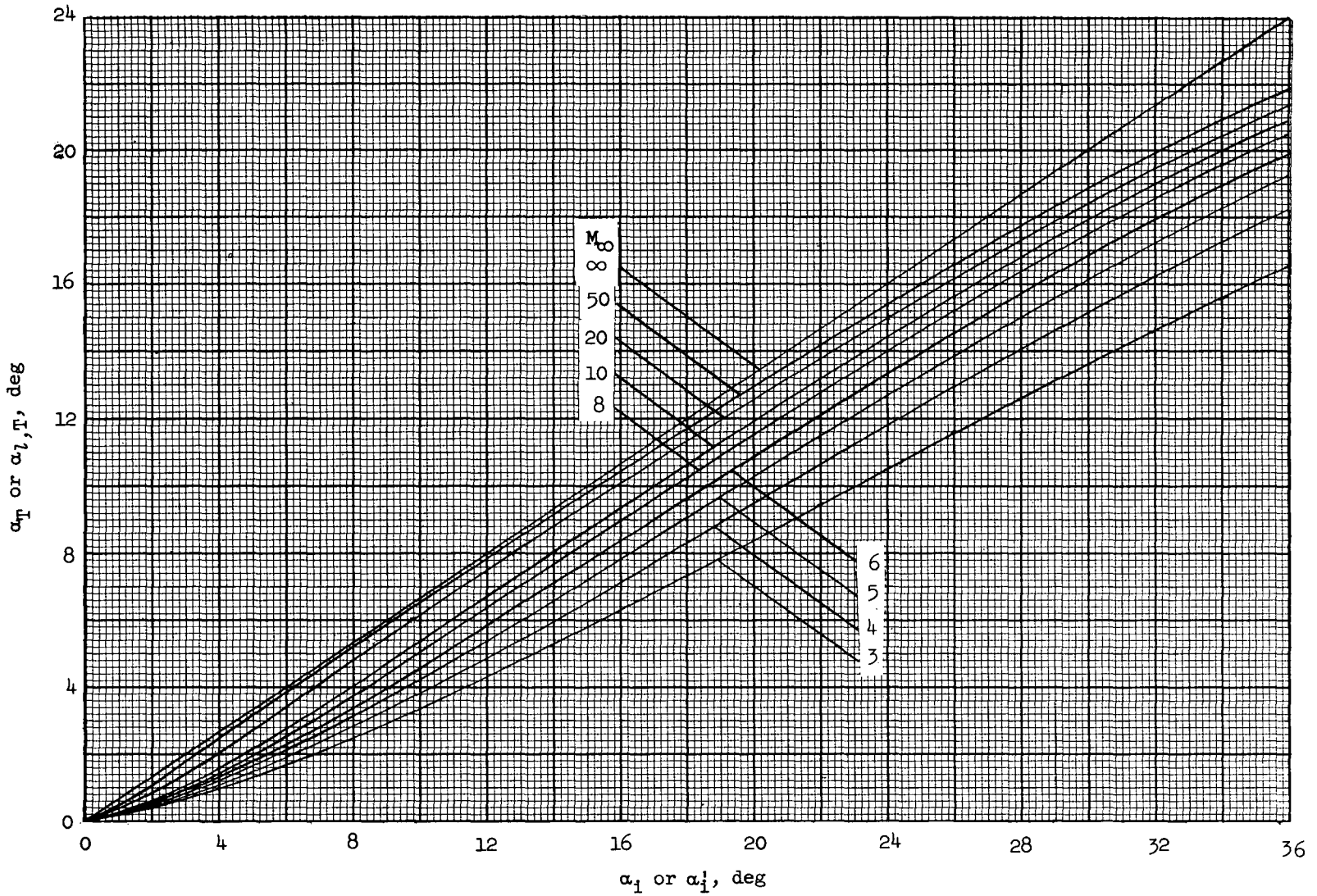

Figure 9.- Variation of α_T with α_i. $\gamma = 1.4$.

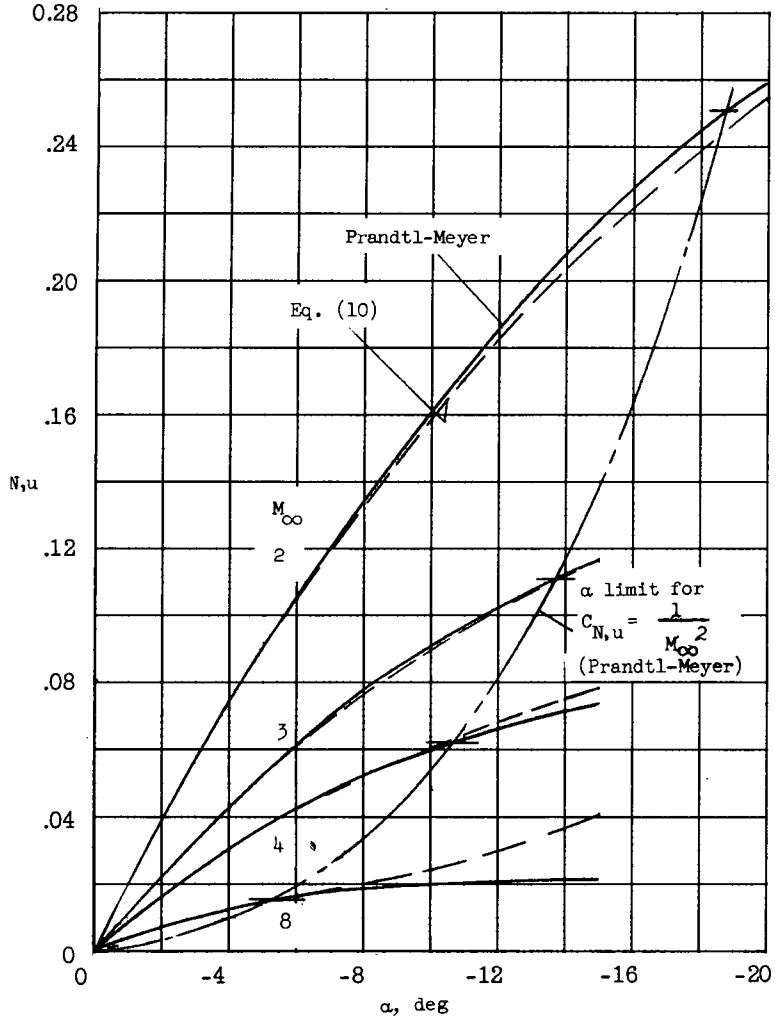

(a) $\gamma = 1.4$.

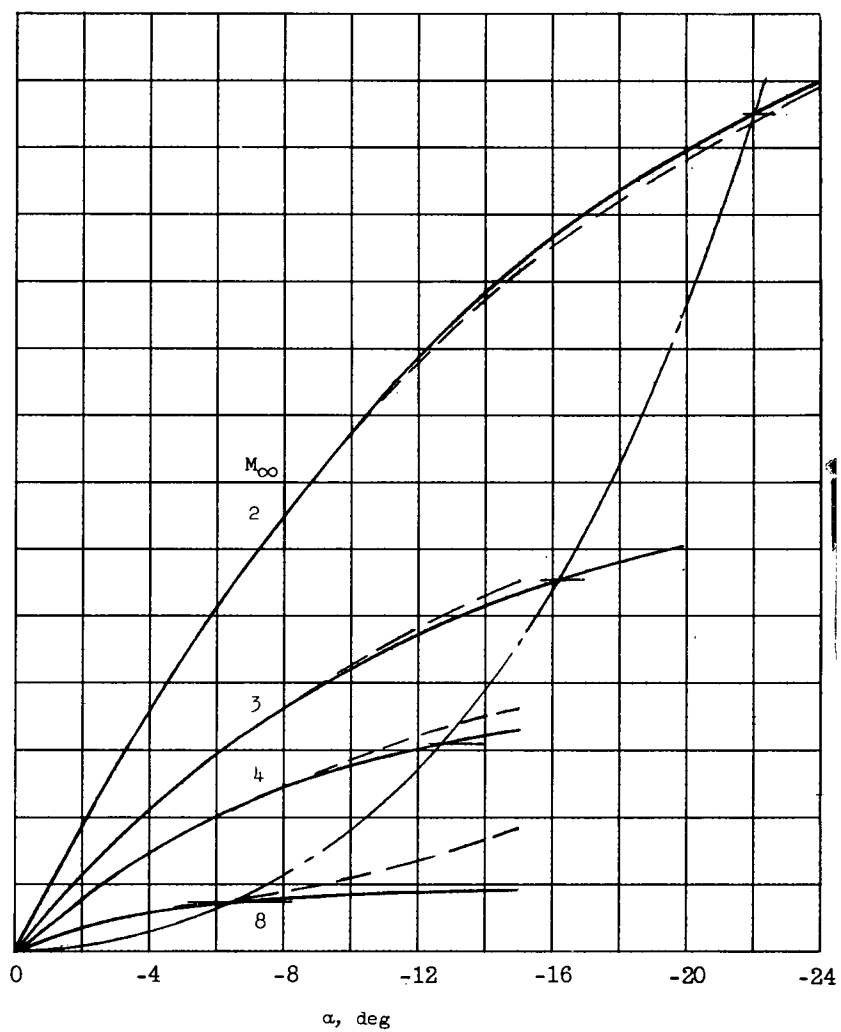

(b) $\gamma = 1.667$.

Figure 10.- Comparison of exact and approximate predictions of variation of two-dimensional flat-plate upper surface normal-force coefficient with angle of attack.

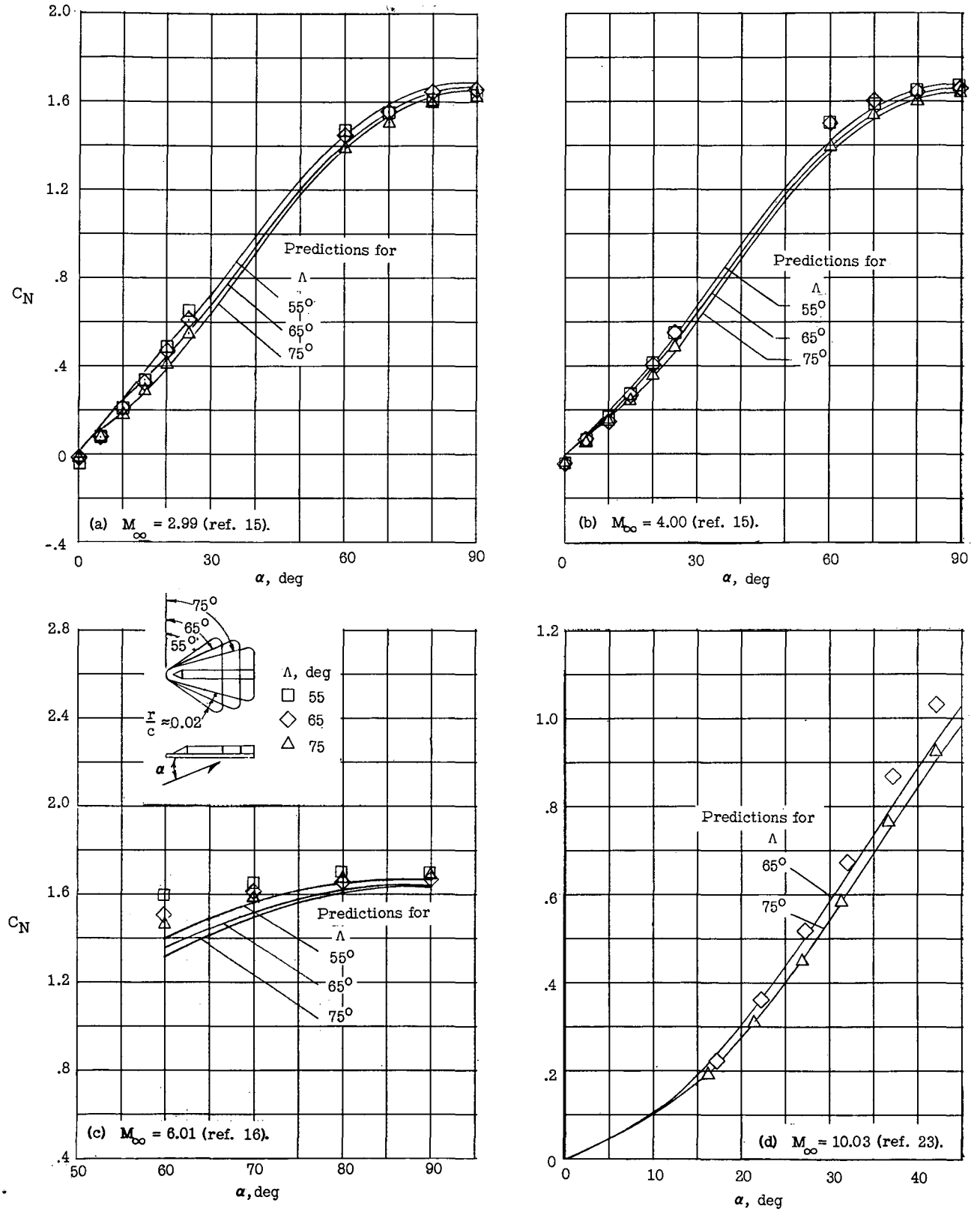

Figure 11.- Comparison of variations of measured and predicted normal-force coefficient with angle of attack for flat delta wings with various leading-edge sweeps at various Mach numbers.

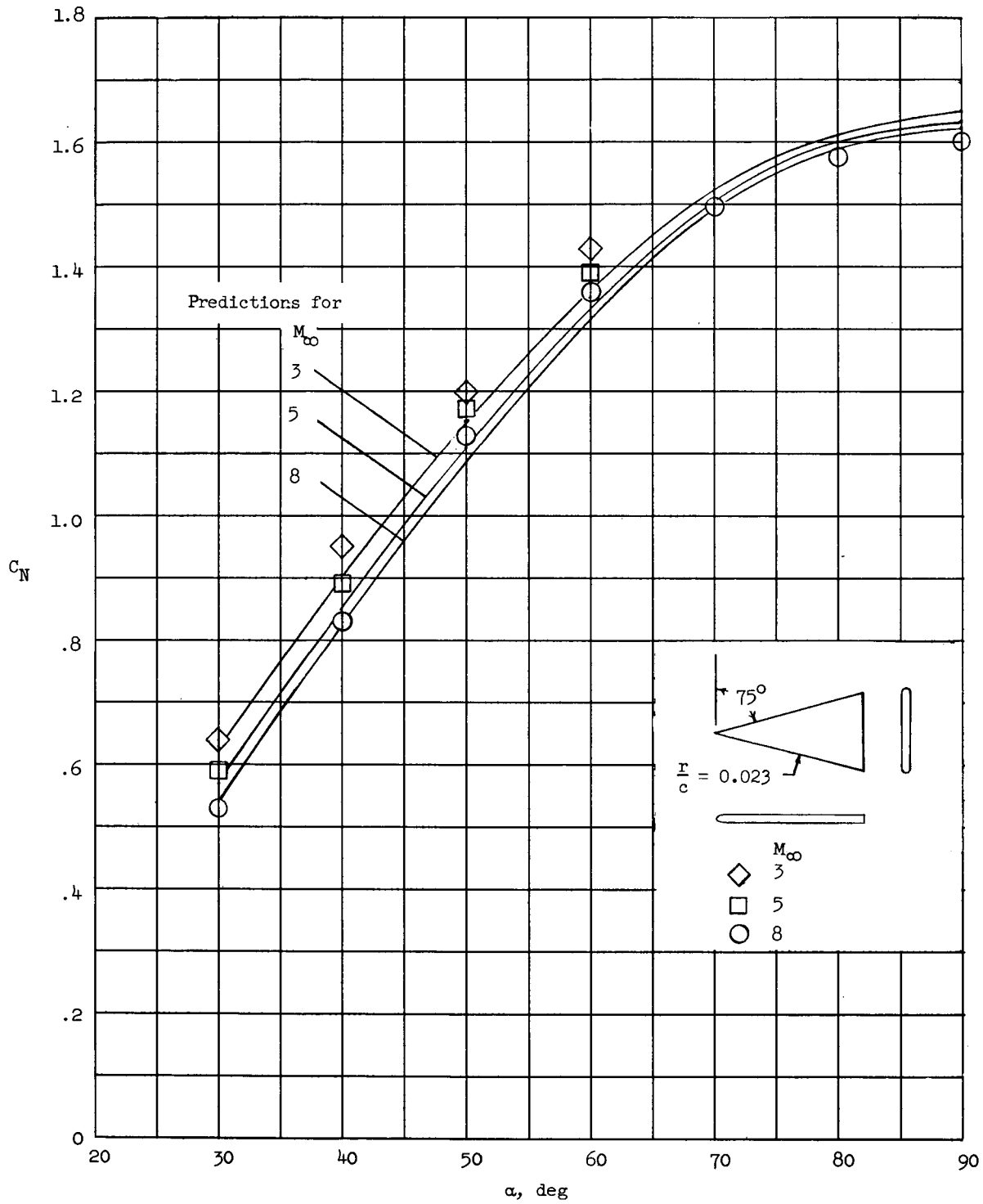

(e) $M_\infty = 3$, 5, and 8 (experimental data from ref. 9).

Figure 11.- Continued.

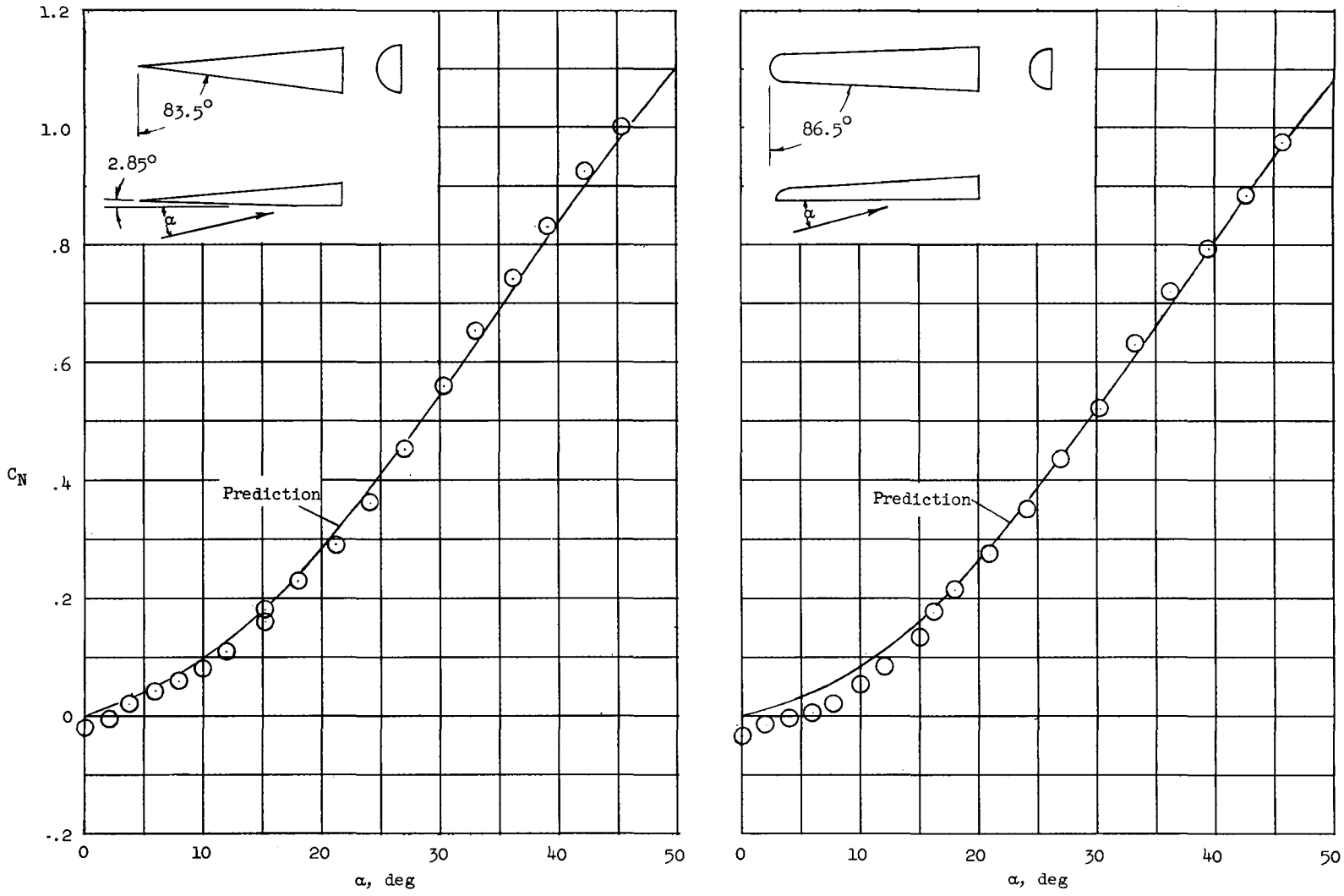

(f) $M_\infty = 8$ (experimental data from ref. 24).

Figure 11.- Continued.

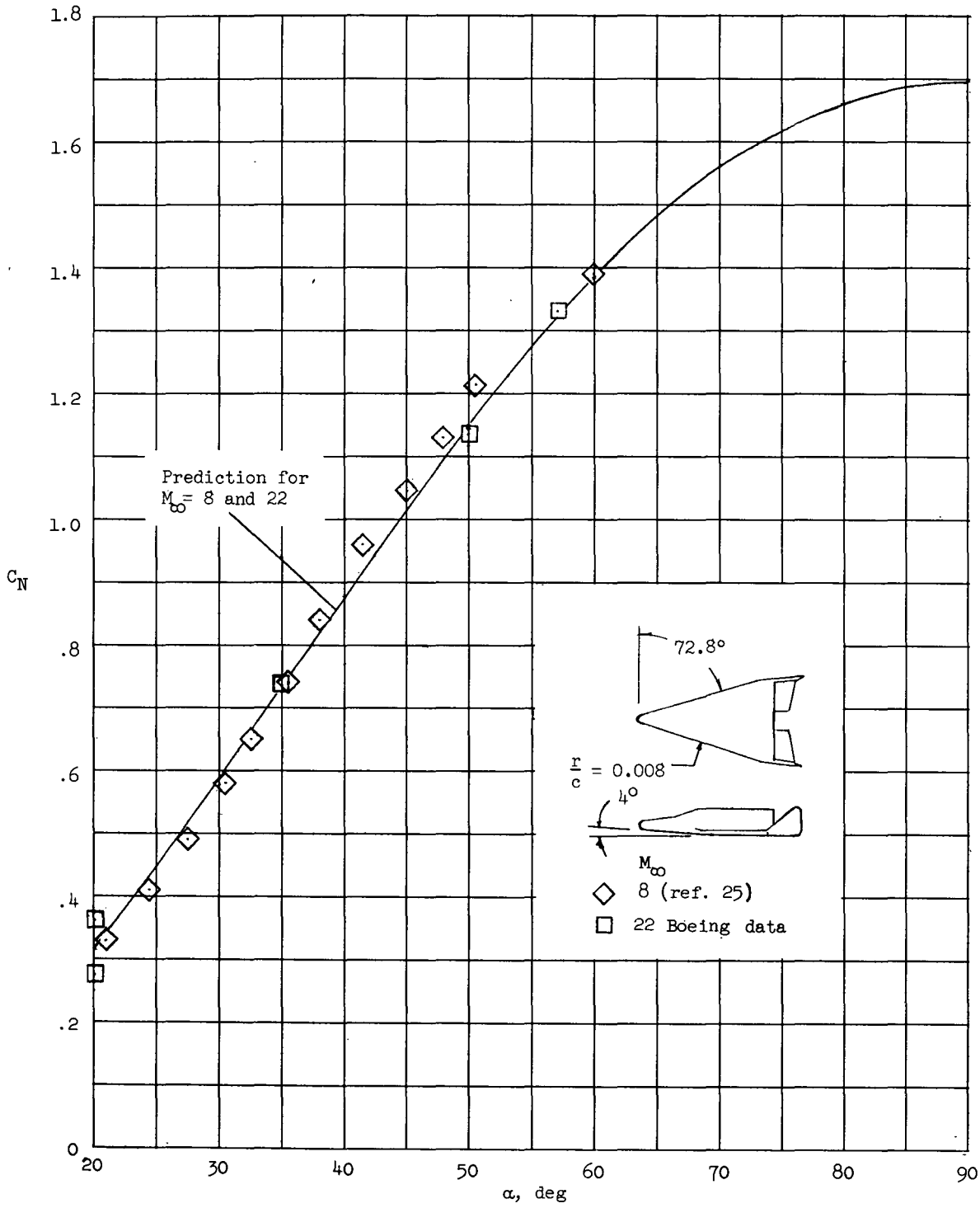

(g) $M_\infty = 8$ and 22.

Figure 11.- Concluded.

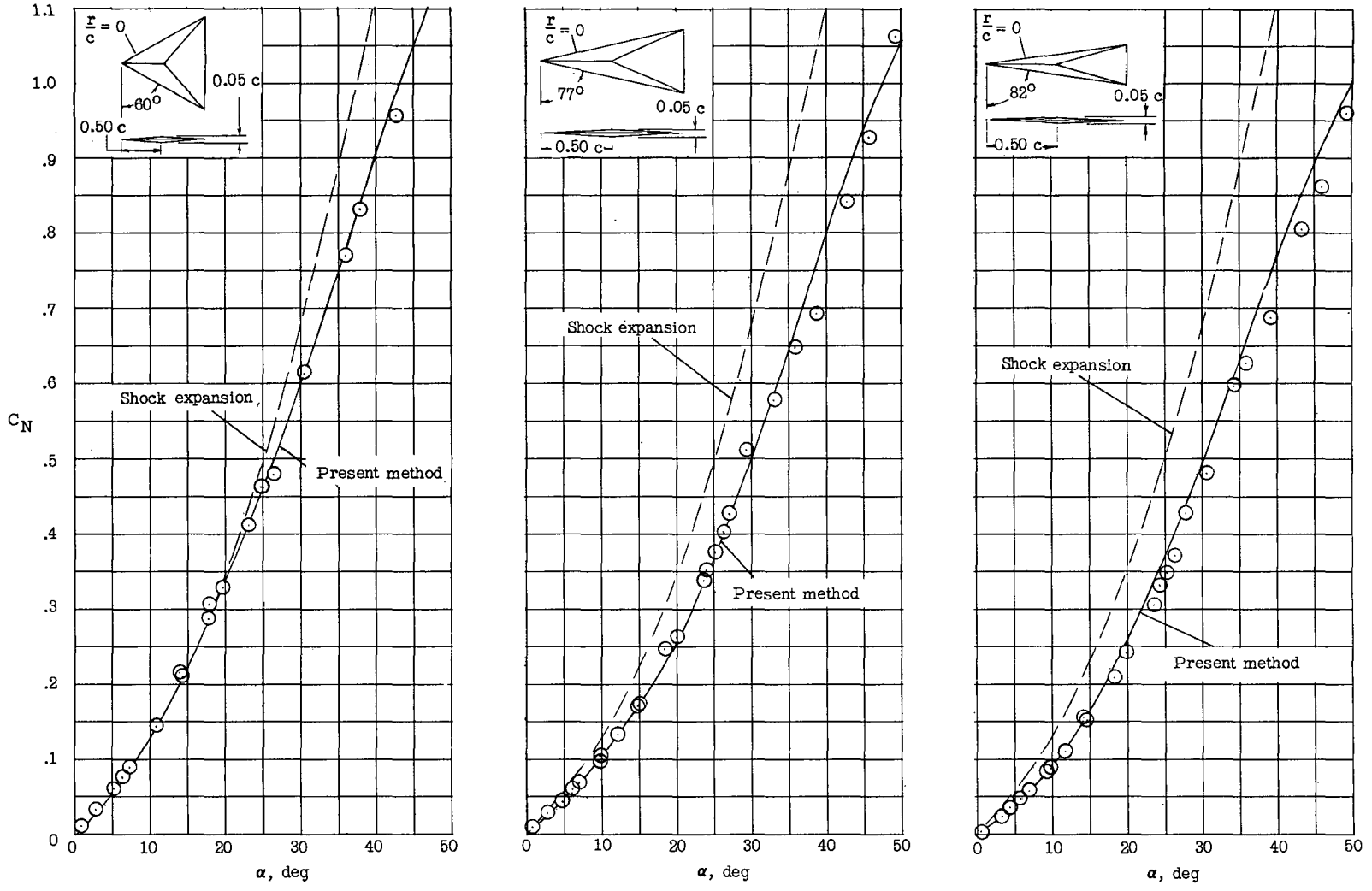

(a) Diamond wings. $M_\infty = 6.8$. (Data from ref. 4 and unpublished data.)

Figure 12.- Comparison of variations of measured and predicted normal-force coefficient with angle of attack for delta wings with dihedral.

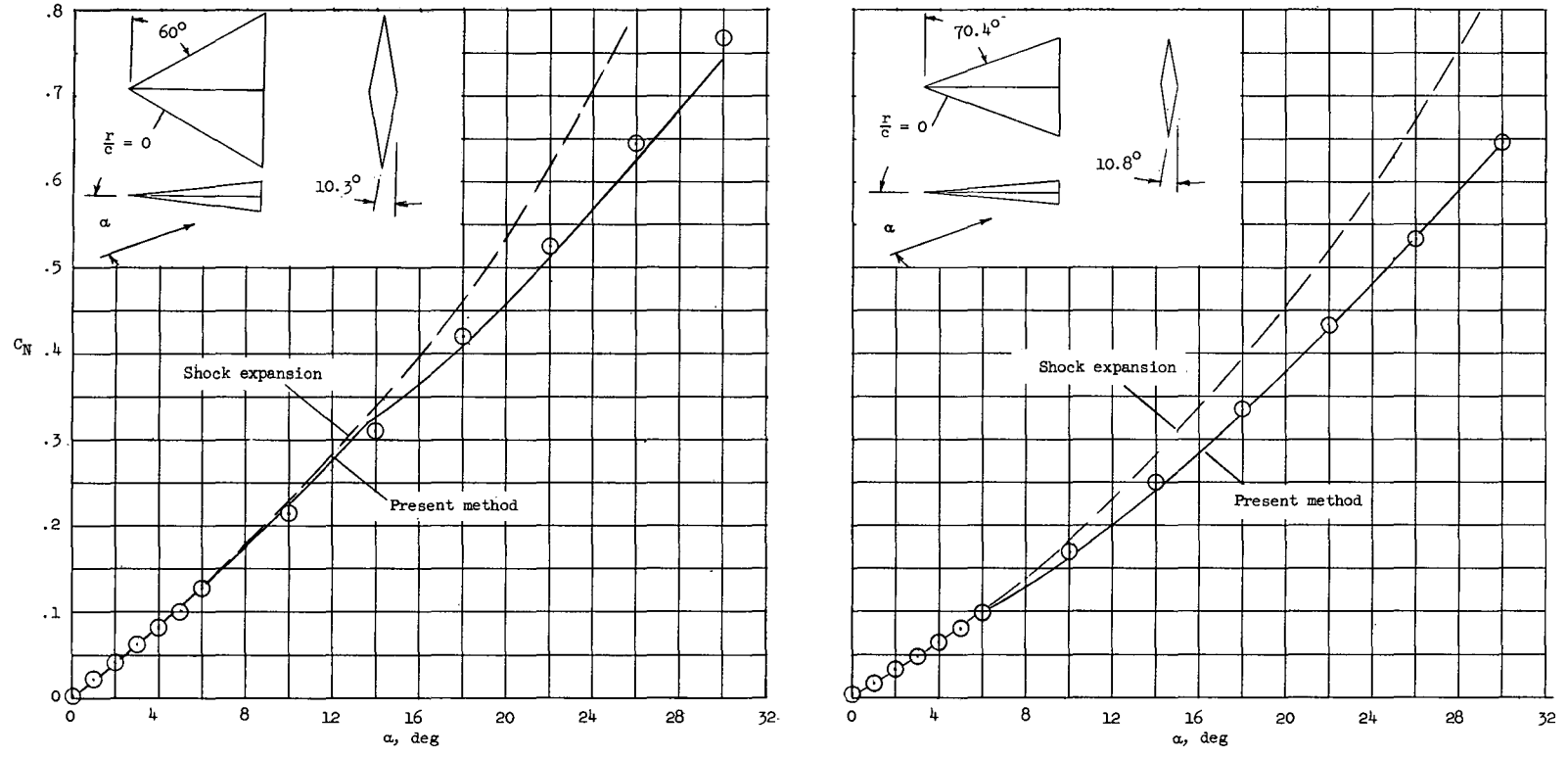

(b) Wedge wings. M_∞=6.8. (Unpublished data.)

Figure 12.- Continued.

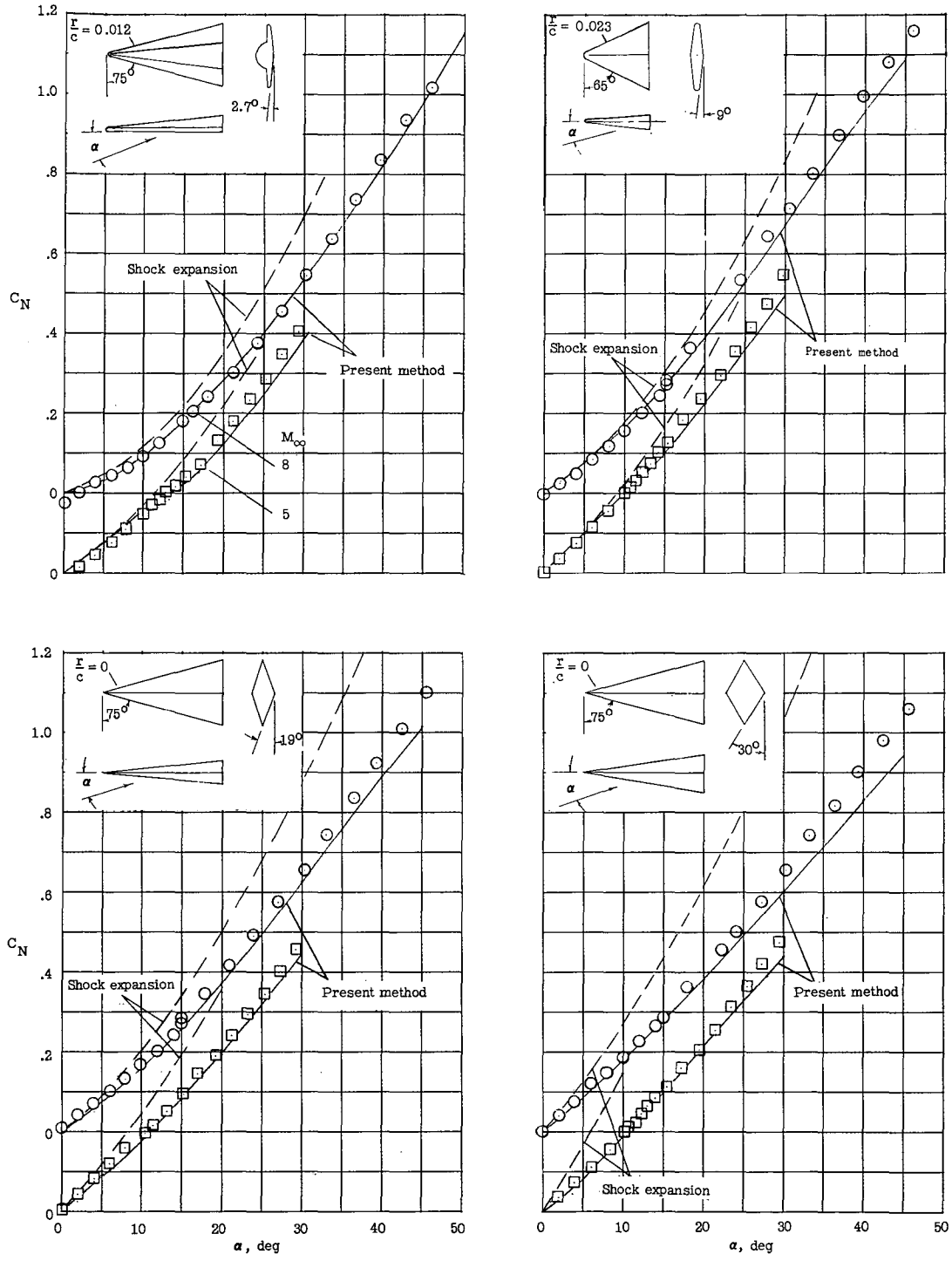

(c) $M_\infty = 5$ (ref. 26) and 8 (ref. 24).

Figure 12.- Concluded.

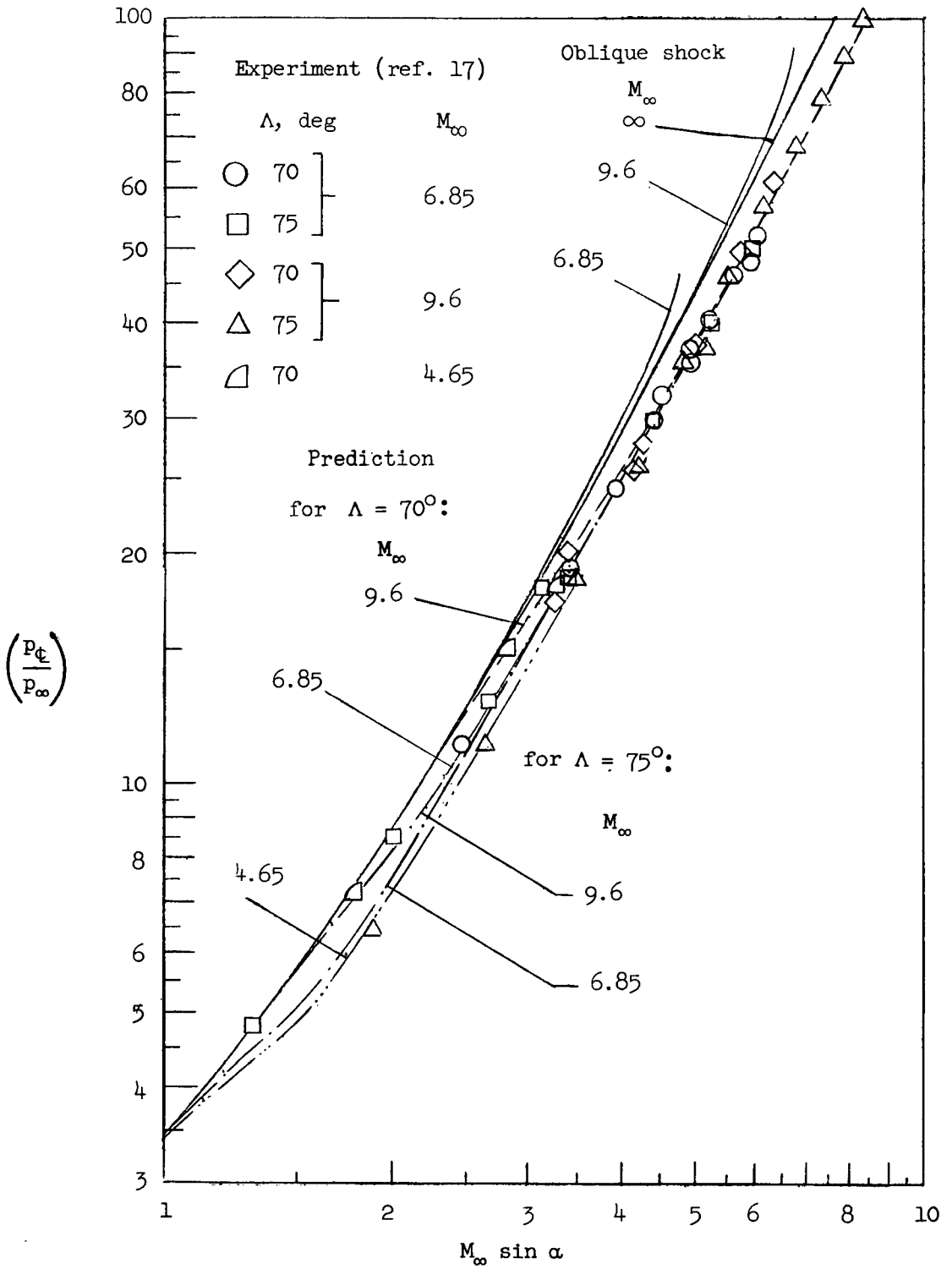

Figure 13.- Comparison of experimental and predicted average ratios of center-line pressure to free-stream static pressure for delta wings of various leading-edge sweeps at various Mach numbers.

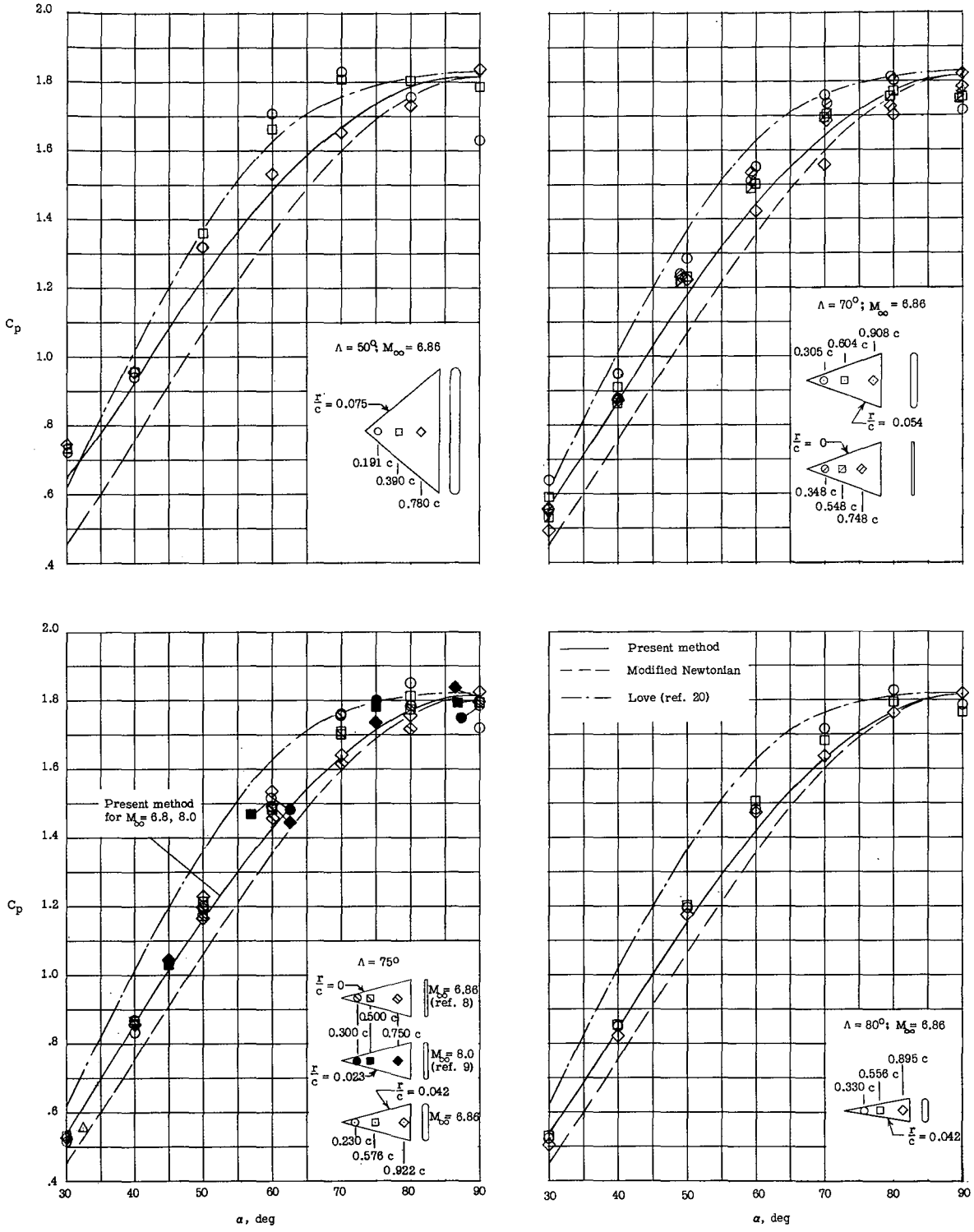

Figure 14.- Comparison of measured and predicted center-line pressure coefficients for flat delta wings of various leading-edge sweeps. Data from unpublished tests except where noted.